Miscellaneous Investigations –100

SUMMARY REPORT ON THE McQUEARY GULCH TRENCH, WILLIAMS FORK MOUNTAINS FAULT GRAND COUNTY, COLORADO

By:
Robert M. Kirkham, GeoLogical Solutions, Alamosa, CO
David C. Noe, Geologist, Paonia, CO
Lauren Heerschap, Real Science Innovations, LLC, Lander, WY
James P. McCalpin, GEO-HAZ Consulting, Inc., Crestone, CO
Shannon Mahan, U.S. Geological Survey, Denver, CO
Matthew L. Morgan, Colorado Geological Survey, Golden, CO

Colorado Geological Survey
2020

SUMMARY REPORT ON THE McQUEARY GULCH TRENCH, WILLIAMS FORK MOUNTAINS FAULT GRAND COUNTY, COLORADO

By
Robert M. Kirkham, GeoLogical Solutions, Alamosa, CO
David C. Noe, Geologist, Paonia, CO
Lauren Heerschap, Real Science Innovations, LLC, Lander, WY
James P. McCalpin, GEO-HAZ Consulting, Inc., Crestone, CO
Shannon Mahan, U.S. Geological Survey, Denver, CO
Matthew L. Morgan, Colorado Geological Survey, Golden, CO

2020

Karen A. Berry
DIRECTOR AND
STATE GEOLOGIST

COLORADO SCHOOL OF MINES
Dr. John Bradford
DEAN OF
EARTH RESOURCES AND
ENVIRONMENTAL PROGRAM

MI-100
DOI: https://doi.org/10.58783/cgs.mi100.hwvk6888

CONTENTS

TABLES

FIGURES

APPENDICIES

PLATE 1

ABSTRACT

In 2005, the Colorado Geological Survey (CGS) conducted a paleoseismic investigation of a scarp in Quaternary deposits at the northern end of the Williams Fork Mountains fault in north-central Colorado. The scarp is located in McQueary Gulch in the northwest part of the Williams Fork Valley. Although this location, at the far end of the fault, was not ideal for a paleoseismic investigation, it was the only feasible location for our study at that time due to budgetary, access, and scheduling limitations. The trenched scarp, herein called the "lower scarp," is located in the hanging wall of the main fault trace at the range front. The lower scarp, 4.8 m high, is 50 to 80 m north-northeast of and downslope from the range front and has a maximum scarp angle of 22.0°.

The main scarp in McQueary Gulch, herein called the "upper scarp," is in Quaternary deposits at the range front. It aligns with a fault-line scarp where Proterozoic crystalline rocks are in contact with sedimentary strata in the Miocene/late Oligocene Troublesome Formation. This 10.8 m-high scarp almost certainly is at least in part tectonic, but a paleoseismic trench across it would require an enormous trench, the cost of which would have far exceeded our budget.

A single slot trench was excavated across the lower scarp and studied during the investigation. Investigators identified six major stratigraphic units and 15 minor subunits based on lithology, genesis, and relative ages. The oldest unit exposed in the trench (unit 1) is the Troublesome Formation, which consists mostly of mudstone and mud-clast mudstone. Units 2 through 6 are composed of late Quaternary sedimentary deposits. The oldest Quaternary deposit (unit 2) is an alluvial unit deposited at the base of the lower scarp. Evidence suggests the lower scarp existed prior to deposition of unit 2, which is Late Pleistocene based on our interpretation of preferred IRSL ages on feldspar in unit 2.

During the deposition of unit 2, the scarp face not only served as the channel wall, but it probably has persisted as a locally prominent topographic feature since the deposition of unit 2. Units 3, 4, and 5 are interpreted either as remnants of late Quaternary mudflow deposits or colluvium deposited on the scarp face, or as slump blocks of bedrock that fell or slid from the scarp face, perhaps into a channel. We were not able to obtain absolute ages for units 3, 4, and 5. Relative dating indicates units 3, 4, and 5 are younger than Late Pleistocene unit 2 and older than unit 6, which is alluvium that spilled down the scarp face during Early Holocene and perhaps latest Pleistocene time, based on OSL dates on quartz from unit 6.

Investigators did not find definitive evidence of late Quaternary faulting or folding in the trench. The trench did contain an impressive structural feature, a long section of north-dipping Troublesome strata that roughly parallels the face of the lower scarp. It then rolls over in an anticlinal or antiformal fold near the upper/southern end of the trench. The trench wall only exposed a few meters of south-dipping beds in the southern limb of the anticlinal fold. Initially, we thought the anticlinal rollover was a minor feature superimposed upon a large monoclinal fold. We now believe it is the crest of an anticlinal feature that we call the Watt anticlinal fold.

Though we did not find conclusive evidence in the trench, our preferred interpretation is the scarp and fold formed at the toe of an unrecognized landslide, or as a transverse ridge within a landslide during or before Late Pleistocene. The upper scarp may coincide with the landslide headscarp and may be both a tectonic and slope instability feature.

Even though this trench did not document evidence of recent fault movement, prior studies by Unruh and others (1993; 1996) and Kirkham (2003) indicate that additional paleoseismic studies of the fault are warranted. The Lost Creek, Middle Mule Creek, and North Battle Creek sites of Kirkham (2003) are more favorable for future paleoseismic studies. A very large trench on the upper scarp at the range front in McQueary Gulch also might yield paleoseismic evidence of late Quaternary faulting.

INTRODUCTION

The Williams Fork Mountains fault is a late Cenozoic structure in north-central Colorado (**Figure 1**). It lies at the western edge of the Williams Fork Valley and eastern base of the Williams Fork Mountains. The fault trends northwest-southeast and juxtaposes Proterozoic rocks in the footwall against Miocene and late Oligocene Troublesome Formation in the hanging wall. Tweto and Reed first identified it (1973) on their 1:62,500-scale map. Later, Tweto and others (1978) incorporated the reconnaissance-level mapping into the 1:250,000-scale Leadville 1° x 2° map. Kellogg and others (2011) included the Williams Fork Valley on their recent 1:100,000-scale map, which was published several years after our McQueary Gulch trench was excavated and logged during 2005.

Tweto (1978, 1979) considered the Williams Fork Valley and Williams Fork Mountains fault as elements of the northern Rio Grande rift system. Unruh and others (1993, 1996) reported geomorphic evidence of Holocene movement along the northern part of the fault based on reconnaissance at a single site. Unruh and others (1993) initially reported a rather high slip rate of 0.3 to 1.3 mm/year for the fault, whereas Unruh and others (1996) subsequently preferred a lower slip rate of 0.1 to 0.3 mm/year.

The studies by Unruh and others prompted a field study of the entire length of the fault by Kirkham (2003) and Kirkham and Lindsay (2003). Due to the dense forest that blanketed much of the fault trace, their investigation involved walking out the fault trace to identify tectonic scarps in Quaternary deposits and measure their profiles. They found numerous scarps of probable tectonic origin in Quaternary deposits along the northern section of the fault, but none were recognized in the southern section (see Figure 3 for locations of their study sites). They also dug soil pits into faulted footwall sediments, at selected locations, and used exposed pedogenic soils to estimate ages of faulted deposits.

Most vertical slip rates determined by Kirkham (2003) and Kirkham and Lindsay (2003) ranged from 0.1 to 0.3 mm/year. In some valleys, scarps cut Quaternary fan deposits of various ages, and scarp heights were progressively higher in increasingly older deposits. This suggests the fault repeatedly ruptured the ground surface during the Quaternary,

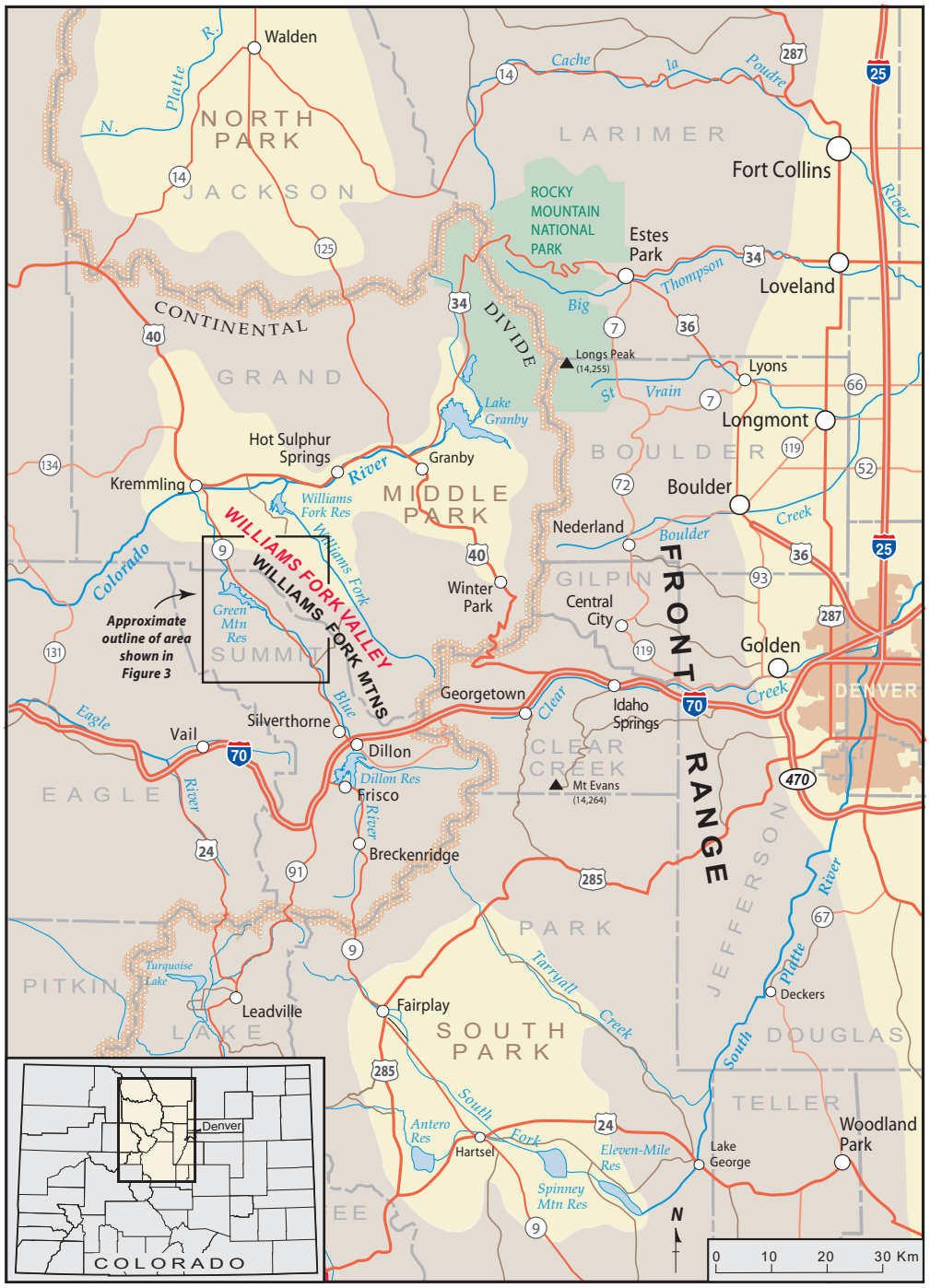

Figure 1 – Regional location map (modified from Kirkham, 2003).

causing moderately large earthquakes (magnitude ~6.5 to 7). The fault probably will cause similar-sized earthquakes in the future.

When a limited amount of funding became available for a short time span in 2005, the CGS undertook a paleoseismic trench investigation in McQueary Gulch during June of that year in an attempt to confirm and expand upon the prior findings of Unruh and others (1993, 1996), Kirkham (2003), and Kirkham and Lindsay (2003). This report describes the observations and conclusions from the 2005 trench investigation in McQueary Gulch.

Only metric units are used in this report, which is the usual format employed in most paleoseismology reports. The following conversion factors may be helpful to readers who prefer English units:

kilometers (km) x 0.62 = statute miles
meters (m) x 3.28 = feet
centimeters (cm) x 0.39 = inches
liters/second (L/s) x 15.85 = gallons per minute.

GEOLOGIC SETTING

The Williams Fork Mountains fault is an east-dipping normal displacement fault that forms the western margin of the Williams Fork Valley graben, one of the northernmost Neogene structural basins within the Rio Grande rift (**Figure 2**). The graben occupies the floor of the Williams Fork Valley, with the Williams Fork Mountains on the west side of the valley and the Vasquez Mountains, a subset of Colorado's much larger Front Range, to the east (**Figures 3 and 4**).

Kirkham (2003) subdivided the Williams Fork Mountains fault into northern and southern sections. Numerous fault scarps in Quaternary deposits exist along the northern section of the fault, which is north of Ute Park. In contrast, Kirkham found no scarps in Quaternary deposits in the southern section, which extends from Ute Park to the southern end of the graben. The paleoseismology trench was excavated across a secondary scarp in McQueary Gulch at the northern end of the northern section of the Williams Fork Mountains fault, about where the fault changes orientation to a westerly trend. No fault scarps were identified in Quaternary deposits along the fault west of McQueary Gulch by Kirkham (2003) and Kirkham and Lindsay (2003).

Syn-rift sedimentary strata, in the Miocene and late Oligocene Troublesome Formation, crop out across the graben floor. The thickness, sedimentology, structural deformation, and exact age of the weakly to moderately lithified Troublesome strata are not well constrained within the Williams Fork Valley. Troublesome strata generally are poorly exposed, have limited known resource potential, and have received relatively little scientific investigation within the valley. Most information on the Troublesome comes from Middle Park, located north of and adjacent to the Williams Fork Valley (Izett, 1968, 1975; Izett and Barclay, 1973; Izett and Obradovich, 2001; Shroba and others, 2010).

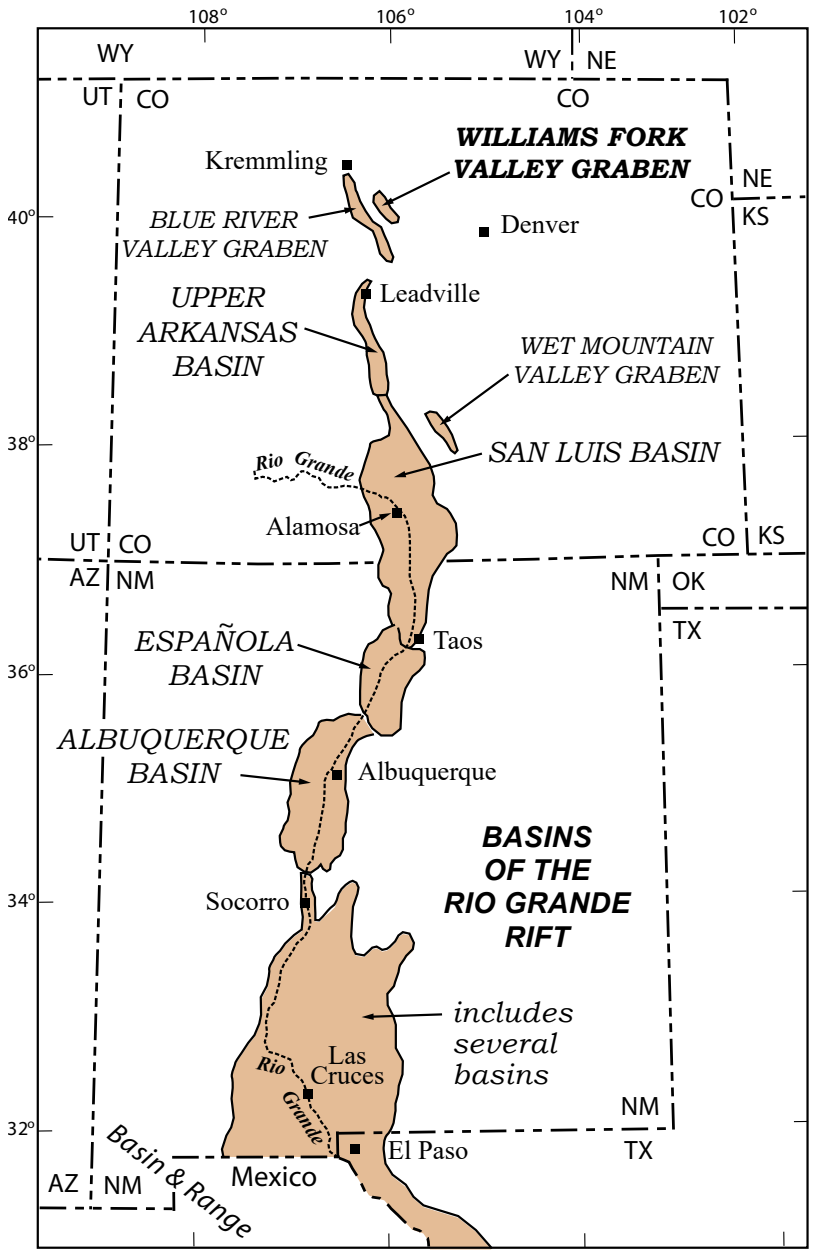

Figure 2 - Map of the major structural basins in the Rio Grande rift. At its southern end, the rift transitions into the Basin and Range Province.

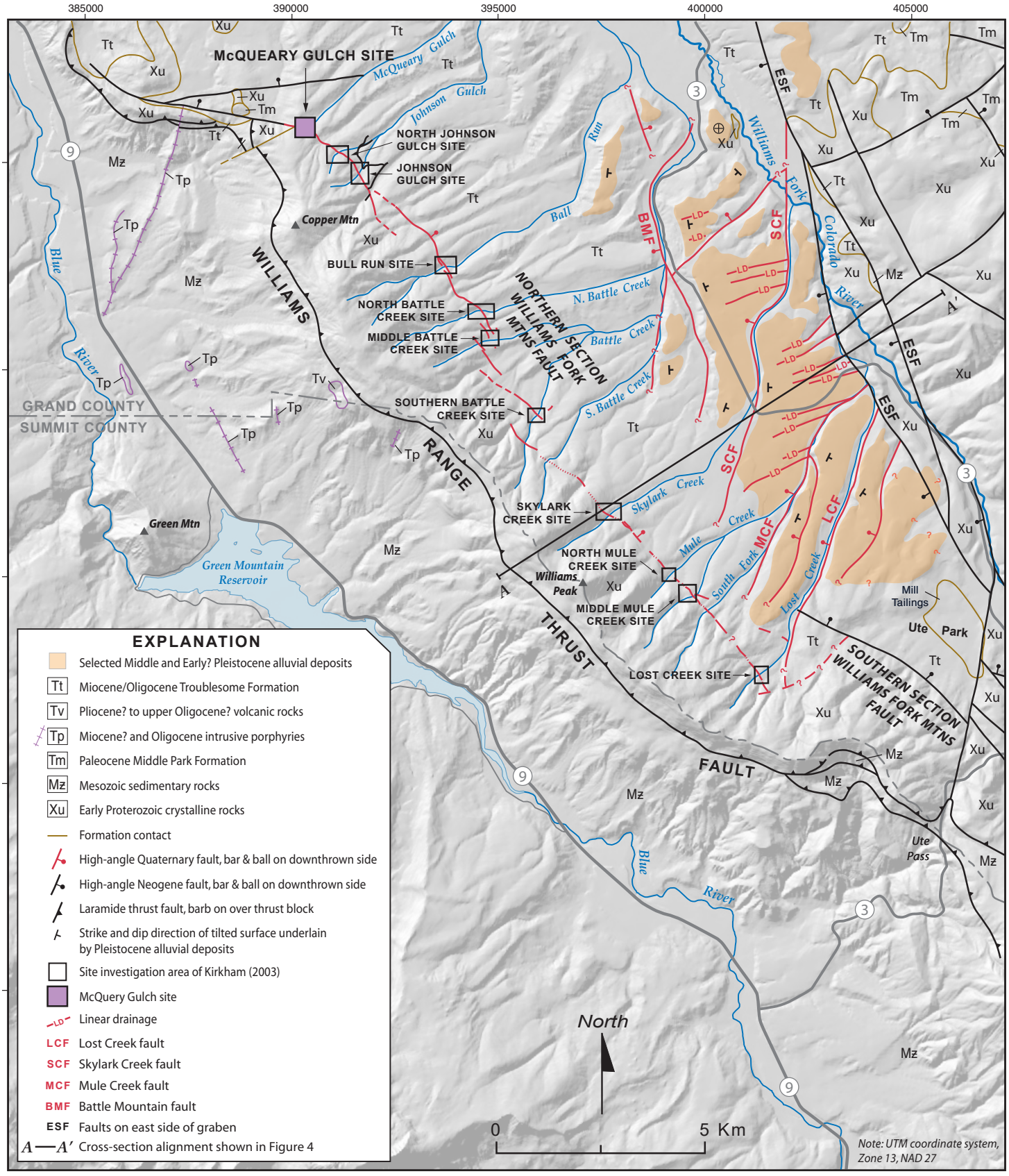

Figure 3 – Simplified geologic map of the Williams Fork Valley and adjacent areas. The McQueary Gulch trench site is at the northwest end of the fault. Refer to Kirkham (2003) for descriptions of fault scarps at other sites denoted by the small black boxes. (modified from Kirkham, 2003).

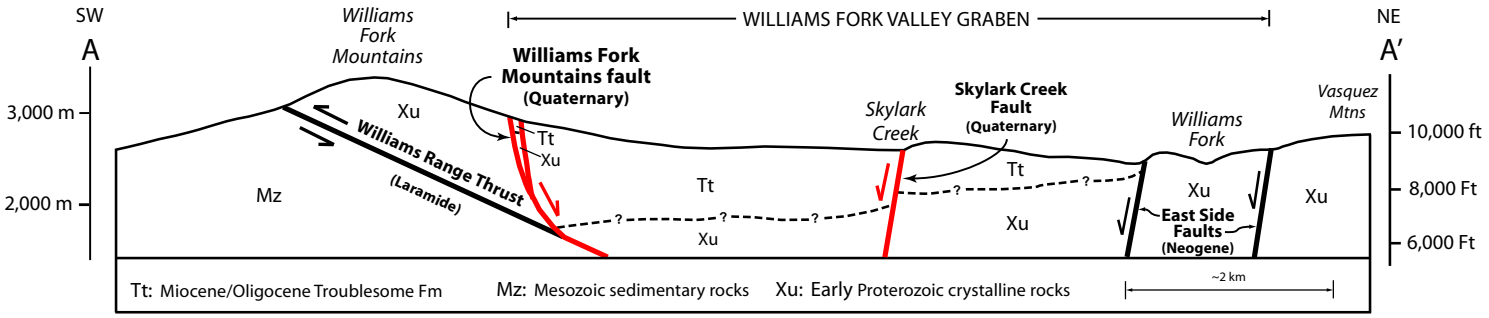

Figure 4 – Generalized cross section A-A', from the Williams Fork Mountains, across the Williams Fork Valley, and into the foothills of the Vasquez Mountains. Thick red lines are Quaternary faults. Thick black lines are Laramide or Neogene faults. Arrows indicate direction of fault movement. See Figure 3 for location of cross section.

Kellogg and others (2011) provide additional information, some of which comes from the Williams Fork Valley, although this report was published several years after our field investigation.

Light-colored tuffaceous siltstone and claystone comprise much of the Troublesome strata. Narrow channels of fluvial sandstone and conglomerate locally are present, particularly in the basal part of the formation, but usually are less than 5 m wide (Kellogg and others, 2011). Beds of air-fall and water-lain tuff also exist within the formation. Izett and Obradovich (2001) described thickness of the Troublesome near the town of Kremmling as about 300 m. Maximum formation thickness in the Williams Fork Valley is unknown. Although a water well located about 2.5 km southeast of McQueary Gulch (permit no. 259071) penetrated 381 m of Troublesome and ended before reaching an underlying formation.

Izett and Obradovich (2001) reported 40Ar/39Ar ages on 32 samples of tuff collected from eight different tuff beds within the Troublesome in Middle Park. Ages ranged from 23.5 ± 0.06 Ma to 6.8 ± 0.03 Ma on these tuff beds, which varied from about 0.5 to 1.5 meters thick. Early Miocene and Oligocene mammalian fossils, including horses, beaver, small rodents, and camels (Lovering, 1930; Izett, 1968, 1975; Kellogg and others, 2011) provide additional age control. Unfortunately, neither the radiometrically dated samples nor the fossils come from strata near the trench site.

The Williams Fork Mountains comprise the footwall of the down-to-east Williams Fork Mountains fault. The mountains abruptly rise up from the valley floor and locally have prominent faceted spurs that face towards the valley, suggestive of Neogene uplift by an extensional fault. Total Neogene displacement across the Williams Fork Mountains fault is uncertain, although, as later described, geologic logs from water wells provide constraints on the minimum vertical displacement in the Copper Creek area. Whether periods of fault activity and inactivity were episodic during the Neogene also is uncertain; we suspect they were.

Early Proterozoic crystalline rocks crop out on the crest and east side of the Williams Fork Mountains. During the Laramide orogeny these rocks were thrust westward over Late Cretaceous Pierre Shale by the west-vergent Williams Range thrust fault, which probably served as the western margin of the Front Range during the Laramide orogeny. Pierre Shale strata crop out on the west side of the Williams Fork Mountains below the thrust plane. As shown in Figure 3, the Williams Fork Mountains fault may sole into the Laramide-age Williams Range thrust fault at depth, an inherited structural relationship found on other normal-displacement faults in the northern Rio Grande rift (Kellogg, 1999).

In plan view, the Williams Fork Mountains fault is not a single trace, but instead consists of a series of en echelon strands whose ends often overlap (Kirkham, 2003; Kellogg and others, 2011). From North Battle Creek to South Battle Creek the overlapping fault traces are right stepping. Water well data available on the Colorado Division of Water Resources website *(http://water.state.co.us/Home/Pages/default.aspx)*, along with geologic mapping by Kirkham (2003) and Kellogg and others (2011) suggest the fault strands overlap in the Johnson Gulch-Copper Creek area, immediately south of McQueary Gulch. **Figure 5** shows the locations of water wells and associated stratigraphic data in this overlap area. Lithologic logs submitted to the Colorado Division of Water Resources serve as the basis of our interpretation of the data shown in this figure.

Water wells between the overlapping fault strands shown in Figure 5 penetrated only 27 to 29 m of Troublesome strata (and overlying surficial deposits) before reaching granitic rocks interpreted as Proterozoic basement rock. East of the eastern fault strand the top of Proterozoic rocks is much lower,

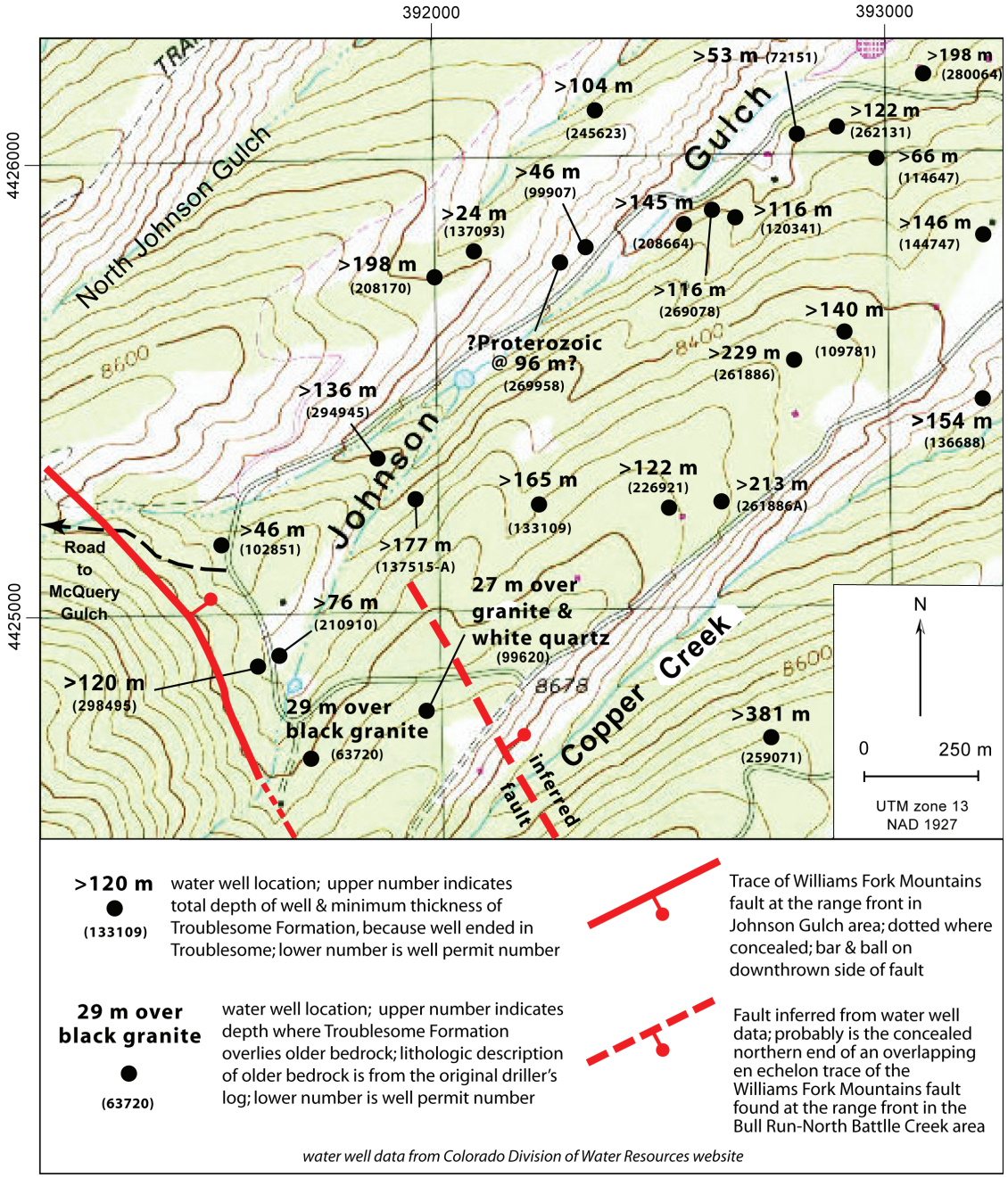

Figure 5 – Map of water well locations used to infer the presence of an additional fault possibly related to the Williams Fork Mountains fault. The authors interpret the additional fault as the concealed northern end of an overlapping en echelon trace of the Williams Fork Mountains fault that lies northeast of the range front in the Bull Run-Battle Creek area. Formations are interpreted from lithologic descriptions in driller's logs for water wells.

and thick sections of Troublesome strata exist there. For example, on the south side of Copper Creek, 381 m of Troublesome strata were penetrated in a well (permit number 25907). The well terminated in Troublesome strata and did not extend deep enough to reach Proterozoic rocks or any other underlying formations that potentially might exist. This evidence indicates the Troublesome is thicker in the Williams Fork Valley than in Middle Park (Izett and others, 2001). Other water wells east of the overlapping fault section encountered 122 to 213 m of Troublesome rocks in the hanging wall of the fault zone, also without encountering any underlying formations or Proterozoic rocks. A similar, rather abrupt thickening of the Troublesome occurs east of the fault trace north of and beyond the overlapping fault section. Whether a similar structural overlap occurs in the McQueary Gulch area is uncertain.Still, if it does, the lower (trenched) secondary

scarp in that gulch potentially could be related to a fault that overlaps the fault strand at the range front.

One water well located in the hanging wall of the fault zone in Johnson Gulch (permit number 268958) reportedly penetrated "Granite tan, soft" at a depth of 98 to 155 m; "Gray granite soft" from 155 to 180 m; "Rose granite" from 180 to 181 m; and "Gray granite, soft" from 181 to 197 m. Although this could indicate a localized structural high, it is equally plausible that the well driller mistook coarse arkosic conglomerate for crystalline bedrock.

Another possible explanation for the water well data involves an outbound concealed fault in the hanging wall of the Williams Fork Mountains fault that is subparallel to the range front fault. Grauch and others (2013) and Watkins (1996) documented an outbound fault in the hanging wall of the Sangre de Cristo fault in the vicinity of Great Sand Dunes National Park and Preserve. That fault is the master down-to-west fault on the east side of the San Luis Basin, a large rift basin that spans the Colorado-New Mexico state line (Figure 2). The outbound fault accommodates much of the total fault displacement on the east side of the San Luis Basin. In contrast, the Sangre de Cristo fault at the range front fault is responsible for significantly less. Whether overlapping fault traces or a subparallel outbound fault exist in McQueary Gulch is unknown, but the presence of two scarps raises that question.

Unnamed, down-to-west Neogene faults bound the east side of the Williams Fork Valley graben, separating Troublesome strata on the valley floor from Proterozoic crystalline rocks in the Vasquez Range to the east (Tweto, 1978; Kellogg and others, 2011). Kirkham (2003) called the two subparallel faults that comprise the major structures on the east side of the graben the East Side faults. Proterozoic crystalline rocks are in fault contact with the Troublesome Formation at the westernmost of the East Side faults, but there is only minor topographic expression of the change in rock type at that fault.

The Vasquez Mountains gradually rise up above the valley floor east of the easternmost branch of the East Side faults. These mountains lack faceted spurs similar to those present locally on the east flank of the Williams Fork Mountains. No evidence of Quaternary movement is documented on the East Side faults. Curiously, rather than establishing a channel in easily eroded Troublesome Formation on the graben floor, the Williams Fork River locally flows in a canyon cut into Proterozoic rock between the two major faults that comprise the East Side fault zone. Perhaps this is a result of superimposition prior to initiation of rift-related extension.

Eventually, the Williams Fork River cuts across the East Side fault zone and enters the floor of the graben where Troublesome strata crop out. This unusual geomorphic relationship between the river and the graben, along with the apparent absence of Quaternary movement on the East Side faults, the gradual topographic rise of the Vasquez Mountains above the faults, and the lack of faceted spurs on the range front, suggest the East Side faults may have had only minor movement during rifting.

As shown in Figure 3, several northeast-southwest-trending, down-to-northwest cross faults extend across much of the graben floor (Tweto, 1978; Kirkham, 2003; Kellogg and others, 2011). They include, from north to south, the Battle Mountain fault, Skylark Creek fault, Mule Creek fault, and Lost Creek fault (Kirkham, 2003). These faults displace Early(?) and Middle Quaternary alluvium, and they terminate against the East Side faults, which suggests unrecognized minor Quaternary movement may have occurred at least locally on the East Side fault system.

No Troublesome strata exist south of an unnamed cross fault that forms the southeast margin of Ute Park (Figure 3). This cross fault may have bounded the southern end of the Williams Fork Valley graben during rifting. Or perhaps Troublesome strata did once exist southeast of the cross fault, but the fault became active late during rifting and the Troublesome strata that formerly existed on its footwall block was removed by erosion. No evidence of Quaternary movement has been reported on the cross fault, although admittedly the geomorphology along much of its trace is disturbed by activities related to the Henderson Mill.

Ephemeral creeks drain the east flank of the Williams Fork Mountains. In many places these creeks have eroded deeply into the Troublesome Formation in the hanging wall of the Williams Fork Mountains fault immediately after crossing the range front fault. For example, at McQueary Gulch the depth of incision immediately downstream of the range front is about 50 to 60 m. A similar amount of incision occurs at Johnson Gulch, and at Copper Gulch the incision attains a depth of about 110 m. Depth of incision increases farther downstream on some creeks. These examples suggest either the rate of incision exceeds the slip rate of the Williams Fork Mountains fault, or that the fault experienced episodic periods of activity.

The drainage basin of McQueary Gulch is bowl-shaped and filled with aspens in the footwall of the Williams Fork Mountain fault at the range front. The bowl-shape and presence of an aspen forest are atypical of most basins at the range front along the Williams Fork Mountains fault. When viewed in Google Earth, the geomorphology of the basin hints at a landslide origin. However, no obvious geomorphic features

typically associated with landslides were observed in the basin during our field work. Nor were other geomorphic features indicative of landslides detected on stereo pairs of ~1:24,000-scale photography, although the thick forest cover inhibited those efforts. The bowl-shaped basin may be the result of a landslide. Shallow groundwater in the basin supports this interpretation. If a landslide did form in the McQueary basin before the late Quaternary, post-landslide erosion and sediment deposition could have subdued its geomorphic features.

TRENCH LOCATION

Based on prior work by Kirkham (2003) and Kirkham and Lindsay (2003), as well as other geologic considerations, the most favorable sites for paleoseismic trench investigations of the Williams Fork Mountains fault are the Lost Creek, Middle Mule Creek, and North Battle Creek sites (Figure 3). The U.S. Forest Service administers these sites, and an extensive permitting process would be required to trench. Additionally, site access crosses both private and public land, through dense forests and steep hill slopes without roads. Acquisition of all the needed permits, landowner consents, and construction of roads would be time consuming, expensive, and perhaps impossible to accomplish. Helicopter access to these more favorable sites was not an option due to cost and safety issues posed by dense tree cover.

Because of scheduling, access, and budgetary constraints, CGS determined the best option was to study a scarp on private land. Land where permission to trench could be arranged promptly and equipment access to the trench already existed. Scarps are present along the Williams Fork Mountain fault at three privately owned sites: the McQueary Gulch, North Johnson Gulch, and Johnson Gulch sites (Figure 3).

At Johnson Gulch, there is a single scarp that can be traced directly to the fault-line scarp at the contact between Proterozoic crystalline rocks and the Miocene/Oligocene Troublesome Formation. However, the site is very narrow, in close proximity to residential structures, and in 2005 was covered by a dense stand of conifer trees. Additionally, a trench at the Johnson Gulch site would be immediately adjacent to a flowing stream. Preventing the stream from flowing into the trench might be a challenge, and ground water seepage into a trench might cause both safety concerns and logistical difficulties.

Two scarps are present at the North Johnson Gulch site. A perennial spring discharges onto the ground surface west of the main scarp, creating wetland conditions on the upthrown side of the main scarp. Also, the ephemeral stream at this site was flowing at the time of our trench study, which would have posed logistic challenges. Severe flooding problems were predicted for a trench at the North Johnson Gulch site.

At the northern end of the fault, the McQueary Gulch site is where fewer and or smaller fault ruptures might have occurred. Yet it was selected for trenching because the onsite access was better, the surface-water and ground-water conditions there were thought to be more favorable, and it was less restrained by topography and forest cover than either the Johnson Gulch or North Johnson Gulch sites. These factors played major roles in site selection for our time-constrained investigation.

Two scarps are present in surficial deposits at the McQueary Gulch site (**Figure 6**). We traced the upper scarp to a fault-line scarp at the range front where Proterozoic crystalline rock is in fault contact with the Miocene/Oligocene Troublesome Formation. A topographically lower scarp exists north-northeast of and about 50 to 80 m from the upper scarp. Past researchers thought the lower scarp is associated with an overlapping en echelon fault, a subparallel outbound fault in the hanging wall of the main fault trace at the range front, or a minor local fault that could provide at least some paleoseismic data for the Williams Fork Mountains fault zone.

The height of the upper scarp is about 10 m in surficial deposits, and the scarp is populated with numerous full-grown conifer trees. A very large, deep "mega-trench" would be required to study the upper scarp, which was beyond the budgetary and time constraints of the project. Additionally, numerous conifer trees populated the upper scarp, trees the landowner wanted preserved.

Our trench was excavated across the lower scarp in McQueary Gulch. Only a relatively small trench was needed. Aspens, which readily re-grow from their roots, were the dominant tree species on this lower scarp. A trench across the lower scarp would not reveal the entire recent slip history of the fault at this location, yet documentation of late Quaternary tectonic activity on the lower scarp would be useful. It could justify additional and more expensive studies at geologically more favorable sites along the fault.

SCARP MORPHOLOGY

Two scarps exist at the McQueary Gulch site, an upper scarp at the range front and a lower scarp about 50 to 80 m north-northeast of the range-front scarp. On the generalized reconnaissance map by Kirkham (2003), the upper scarp at the range front and the lower scarp are subparallel. In contrast, our detailed mapping of the trench site (Figure 6)—utilizing a GPS receiver to locate mapped features—depicts the scarp at the range front as concave to the southwest and following the contact between Proterozoic rocks and the Troublesome strata.

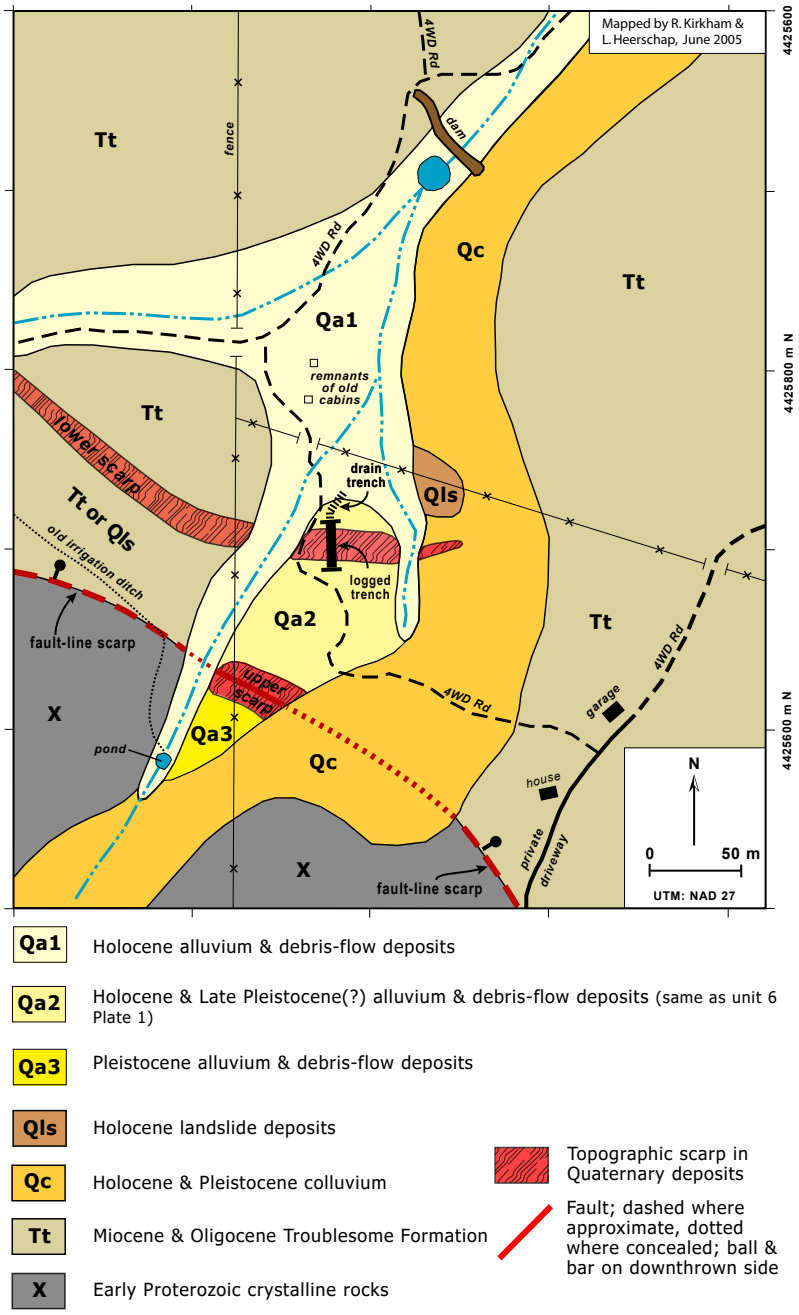

Figure 6 – Geologic map of the trench site in McQueary Gulch.

In contrast, the lower scarp is concave to the northeast and has Troublesome strata on both sides. To the south-southeast, the upper scarp continues to follow the fault-line scarp at the range front, whereas the lower scarp projects towards a saddle on a ridge formed in Troublesome strata on the southeast side of McQueary Gulch. However, the lower scarp terminates in colluvial deposits before reaching the ridge.

Kirkham (2003) measured topographic profiles of both the upper and lower scarps. The profile of the lower scarp, which we trenched during the current investigation, is shown in **Figure 7A**, and a photograph of it is in **Figure 8**. The lower scarp is 4.8 m high, has a surface offset of 3.5 m, and maximum scarp angle of 22.0°, which is at the lower range of scarp angles measured by Kirkham (2003) at other locations along the Williams Fork Mountains fault. Profile irregularities on the upthrown side of the lower scarp at ~40 m from beginning of profile reflect disturbances related to the jeep trail that accesses the trenched area. As shown on Figure 6, map unit Qa2 exists on both sides of the scarp, whereas the scarp is cut out and covered by unit Qa1.

Figure 7B shows the profile of the upper scarp at the range front. Height of the upper scarp is 10.8 m, the surface offset is 5.8 m, and the maximum scarp angle is 19.5°. A paleoseismic investigation of the upper scarp requires a much larger trench, which was beyond the scope of our project.

TRENCH LOGISTICS AND EXCAVATION

The McQueary Gulch trench is located on privately owned land in the NE/4 NW/4 of trapezoidal-shaped section 18 in T.1S., R.79W. Excavation of the slot trench initiated on June 6, 2005. The landowner dug the trench using a Caterpillar 225 trackhoe. The excavation started near the upper (south) end of the scarp and proceeded northward down the scarp face and beyond the toe of the scarp. The contractor installed aluminum bracing shores as the excavation progressed. In the first 10.3 m of the excavation, minor inflows of ground water (<0.063 L/s) seeped from the base of three shallow channels, each of which consisted of sandy gravel. A major ground-water seep with an inflow rate estimated at 1.5 to 2 L/s issued from Troublesome mudstone at the bottom of the trench about 10.5 m from its upper end. Minor caving affected the lower 1 to 1.3 m of the trench wall north of the major seep. We installed new shores to support the unstable trench walls for several meters north of the large seep. The seep continued to cause stability problems throughout the project.

During the night of June 6, the trench filled with water and a relatively large section of the west wall failed, even though the contractor installed shoring. On June 7, the contractor removed displaced shoring and dewatered the trench using a trash pump. The pump ran for about 10 to 15 minutes before breaking down. A decision was made to continue

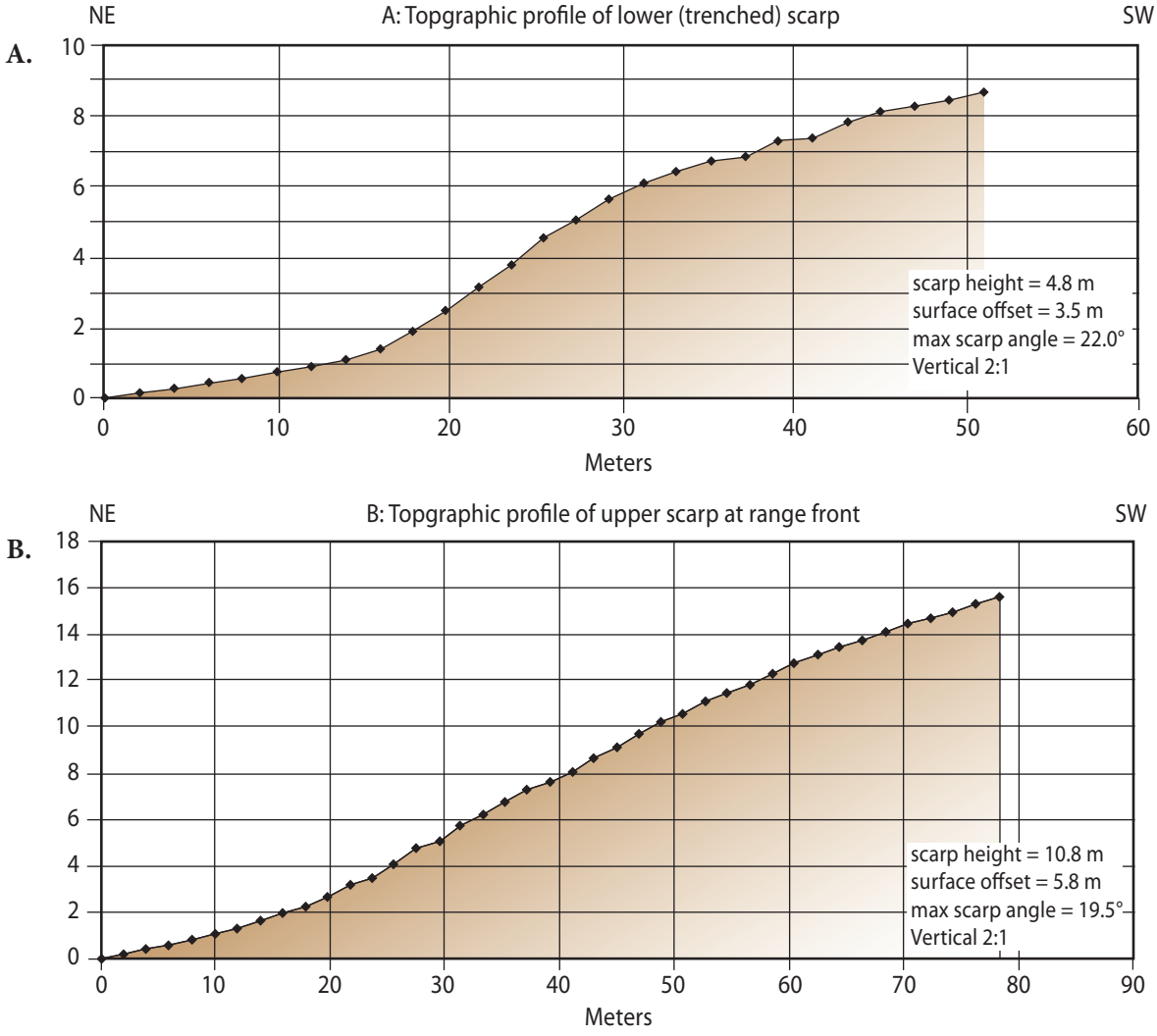

Figure 7 – Topographic profiles of scarps in McQueary Gulch. A: profile of the lower scarp, which was trenched; B: profile of the upper scarp at the range front. See Kirkham (2003) for location of profiles.

the excavation farther down the hillslope, gradually reducing the depth of the trench, yet maintaining a northward-sloping trench floor (**Figure 9**). This allowed water in the trench to drain away from the area to be logged. The trench was about 1.5 m deep at the end of the shored section and gradually became shallower until the trench floor intersected the ground surface. The orientation of the extended trench was modified so it was parallel to the slope of the ground surface, which allowed the trench to daylight in the shortest possible horizontal distance. After completion of trench logging, the trench was backfilled during the late afternoon of June 17, 2005, using a small bulldozer.

The south end of the trench (log coordinate 0 m H on **Plate 1**) is at UTM 390475 m E and 4425690 m N (Zone 13, NAD 27). The trench extended from there in a N3°W orientation (Azimuth 357°) for about 30 m, at which point it changed to N20°E orientation (Azimuth 20°) and continued for about another 20 m to where it daylighted at the ground surface. Ground water that seeped into the trench flowed by gravity out of the north end of the trench.

The east wall of the shored trench section was selected for logging because it was intact and had nearly vertical walls, in contrast to the west wall, which had partially failed and was more irregular. We cleaned the east trench wall by hand. Using a tape measure and self-leveling level, researchers established a one-meter stringline grid on the southern 23 m of the east wall . They secured vertical stringlines at the ground surface, and a small rock was tied to the bottom of the stringline and suspended above the trench floor. The horizontal stringlines were secured to the trench wall using 10-inch-

Figure 8 – View of the lower scarp looking east, at the trench location. Person is standing at the base of the scarp.

long spikes. We used duct tape to attach the vertical and horizontal stringlines at their intersections, and labeled the grid coordinates on many of the stringline intersections.

In the field, researchers labeled the grid system using a method frequently employed by civil engineers on grading projects. However, grading projects typically use English units, whereas we used metric units. We also established a grid coordinate 0+00 m H and 0+00 m V at ground level at the upper (southern) end of the east trench wall. We labeled each vertical stringline consecutively, starting at 0+00 H, then proceeding 1 m to 1+00 H, 2 m to 2+00 H, etc. Researchers also labeled each horizontal stringline consecutively, starting at 0+00 V, then -1+00 V, -2+00 V, etc. Negative numbers on the horizontal stringlines indicate the depth below the starting point of the grid. The number to the left of the "+" indicates the horizontal or vertical distance in meters from the starting point of the grid, and the numbers to the right of the "+" indicates the distance in centimeters beyond the last even-meter stringline. At the request of a peer reviewer, we converted the civil engineering grid numbering system to a decimal system for this report. Hence, stringline 1+00 H, -2+65 V becomes 1 m H, -2.65 m V on the trench log (Plate 1).

Figure 9 – View looking south across the trench. The shored part of the slot trench was logged, with the extended part of the trench needed to dewater the trench. Large inflows of groundwater initially entered the trench. The inflow gradually diminished, tapering off during succeeding days and when backfilled was nearly dry. The shift in trench orientation in the foreground was needed to daylight the trench with the shortest horizontal distance.

In wet sections of the trench, CGS laid planks on horizontal members of adjacent shores, and used them to work on. As the logging proceeded, water flowing from the major seep gradually reduced to less than 0.2 L/s, and the floor of the trench slowly dried. This allowed for manual excavation of a narrow slot 0.2-0.5 m below the original floor of the trench to expose critical geologic relationships. Field staff dug a shallow pit using shovels at the base of the east wall at 26 m H, 3 m beyond the logged section, in an unsuccessful attempt to expose the top of the Troublesome Formation.

Nails with small pieces of colored flagging were pinned to the trench wall to mark contacts, bedding planes, and other items of geologic importance. Kirkham and Noe were responsible for most of the geologic interpretations and placement of the nails. McCalpin reviewed their interpretations and made several recommendations during the afternoon of June 15 and all day on June 16. Kirkham and Heerschap recorded the top and bottom of the trench, the position of the shores, and all geologic information on gridded paper at a scale of 1 inch = 1 meter.

Researchers measured structural attitudes of contacts in the Troublesome Formation, where the contact was visible on both trench walls. Channel orientations in unit 6 were measured where the channel thalweg, channel margin, or channel edge was apparent on both trench walls.

Photographs of the geologic features, exposed in the narrow slot trench, are poor quality and are not included in this report. Factors contributing to the poor photographic documentation included not only the narrowness of the trench and obstructions caused by the support shores and planks that spanned the shores, but also the poor lighting conditions caused by overcast skies from which frequent rain and occasional snow fell.

TRENCH GEOLOGY

Plate 1 contains the trench log, prepared from exposures on the east wall of the trench. The trench log shows color-coded stratigraphic units, areas of bioturbation and burrowing (krotovina), and trench shores, with contact lines, symbols, and notations for surficial soil horizons, structure, channel orientations, ground water seeps, and age-dating sample locations.

Stratigraphy

The authors recognize six major stratigraphic units (units 1 through 6) in the trench and further divide units 1, 2, and 6 into minor stratigraphic subunits. Appendix A contains detailed descriptions of all of the stratigraphic subunits.

Unit 1: The oldest deposits in the trench (Unit 1) are weakley consolidated sedimentary bedrock correlated with the Miocene and late Oligocene Troublesome Formation. The Troublesome Formation is subdivided into seven subunits in the trench. In ascending order, the subunits are labeled 1a through 1g. All Troublesome subunits except subunit 1b are mudstones with varying amounts of clay, silt, sand, angular clasts of mudstone, and sparse clasts of crystalline rock. When dry, most of the Troublesome has a slightly chalky appearance. This suggests the strata contain varying amounts of volcanic ash or altered volcanic ash, as do strata in the Troublesome in adjacent areas (Izett, 1968; Izett and Barclay, 1973).

The Troublesome mudstone subunits commonly include sparse to abundant angular clasts of mudstone that are lithologically similar to the surrounding matrix and range up to about 5 cm in diameter. Some of the mudstone units contain thin limonitic beds of siltstone or very fine sandstone that are used locally to subdivide the formation into the subunits. Where the limonitic beds pinch out, units 1c through 1f merge. Subunit 1b consists of a single long, thin lens of fluvial sediment that extends from 8.70 m H where the channel abruptly terminates against mudstones of the Troublesome Formation to 17.20 m H, where it is cut out by a younger channel (unit 2) in surficial deposits. Subunit 1b becomes finer grained from south to north, ranging from clast-supported sandy pebble conglomerate at 9 m H to slightly pebbly, clayey very fine sand near 16 m H.

The upper ~1 m of Troublesome strata exposed in the trench is weathered, mostly to clay. Unweathered Troublesome strata typically are blocky. The base of the weathered bedrock, shown on Plate 1 between 4 m H and 11 m H, cuts across the bedding and is roughly parallel with overlying strata at both the base and top of unit 6.

Units 2 through 6 are Quaternary surficial deposits.

Unit 2: Unit 2 is the oldest surficial unit exposed in the trench. Unit 2 is found in a channel at the base of the scarp. It was probably was deposited during the late Quaternary after the scarp had formed. We interpret it as stream alluvium and debris flows associated with the modern drainage to the west and north of the trenched scarp. The authors recognize three minor subunits in unit 2. In ascending order, they are subunits 2a, 2b, and 2c, all of which onlap onto and terminate against the channel margin cut into the Troublesome Formation. All three subunits contain varying amounts of gravel

composed of Proterozoic lithologies. Erosion associated with the unconformity at the base of unit 6 removed the uppermost sediment in subunit 2c.

Subunit 2a is a clast-supported fluvial deposit of sandy gravel that coarsens northward. Clasts are subround to subangular. Subunit 2b is a matrix-supported, slightly gravelly sand interpreted as a debris-flow deposit. Likely deposited during a mudflow, subunit 2c is chiefly sandy or pebbly clay with angular clasts. Stratigraphic relationships suggest unit 2 was deposited after at least part of the scarp formed.

Unit 3: In the trench, we encountered a single deposit of unit 3 on the margin of the channel that contains unit 2. This block of mud-clast mudstone is lithologically similar to beds within the Troublesome Formation (unit 1). However, iron-stained beds within the block indicate it is structurally discordant with the adjacent in-place Troublesome bedrock. The authors interpret unit 3 as a block of Troublesome Formation that broke loose from the unit 2 channel margin and slumped into the channel over unit 2c.

Unit 4: A single deposit of unit 4 overlies unit 3. It consists of micaceous, sandy, silty clay with scattered angular pebbles composed of mudstone and Proterozoic lithologies. The authors interpret this unit as either a locally derived mudflow deposit or colluvium eroded off the scarp. The deposition of unit 4 occurred in a channel cut into unit 3. Erosion of the top of unit 4 occurred before the deposition of overlying unit 5.

Unit 5: The trench exposed five disconnected deposits of unit 5. All are micaceous silty clays with varying amounts of widely scattered, angular to subangular pebbles and cobbles composed of Proterozoic lithologies. The largest deposit of unit 5, which occurs between 15 and 20 m H, rests on an erosion surface cut into units 1f, 2c, 3, and 4. Three deposits of unit 5 occur on the north side of channel-like step-downs cut into subunit 1f. The fifth deposit rests on unit 1f on the south side of the anticlinal fold in Troublesome strata.

Unit 5 probably was deposited as one or more mudflows, or as colluvium. Since an erosion surface (or surfaces) overlies and truncates the tops of all five separate deposits, it is uncertain whether they were once part of a single deposit or if they represent multiple episodes of deposition. The base of each deposit is progressively higher than the next deposit to the north, which suggests the deposits may be eroded remnants of colluvium derived from the scarp. The scarp face was modified by erosion after deposition of unit 5 but before deposition of unit 6.

Unit 6: unit 6 is the youngest deposit in the trench. It corresponds to unit Qa2 in the geologic map shown in Figure 6. The authors subdivided unit 6 into two subunits. Subunit 6a, which constitutes nearly all of the unit 6 sediment exposed in the trench wall, consists of gravelly sand and lesser amounts minor sandy gravel, with occasional discrete mud drapes. It was present across the entire logged section of the east trench wall. The deposition of subunit 6a likely occurred as a series of amalgamated hyperconcentrated floods.

Gravel clasts in subunit 6a range in size from granules to large cobbles and are composed nearly entirely of subangular Proterozoic lithologies. We observed a single sharp-edged flake of banded chert in subunit 6a at 14.10 m H. Sediments in the subunit are poorly sorted, which makes discerning bedding challenging. Clast-supported gravel bars are locally present, but we could not trace more than a meter laterally. We noted a few discrete mud drapes in some channels; the color of the mud is similar to that in the Troublesome Formation.

The channeled base of subunit 6a rests on an unconformity cut into all underlying units and extends across the entire length of the logged trench. The channels progressively step-down in elevation across the scarp. Where the underlying units are older mudstones or gravelly clays, the authors were able to identify channel thalwegs and margins. The southern margin of most channels is steeper than the northern margin. From the top of the scarp to 14.50 m H, the channels are visible on both trench walls. Measured orientations of the channel thalwegs and margins suggest the channels in this part of the trench obliquely crossed the scarp (azimuths ranged from 62 to 74°; dips varied from 5 to 10° NE). Channel thalwegs and margins internally within unit 6a were impossible to discern due to the absence of internal bedding.

In the lower part of the trench, from 14.50 m H to end of the logged trench, the channel features in subunit 6a exposed on the east wall of the trench do not match up with similar channel features on the west wall. In the lower part of the trench, it appears deposition of subunit 6a sediments occurred in channels that flowed down the scarp, not obliquely across it.

There are three discrete, isolated deposits of subunit 6b in the trench at 4 m H, 9 m H, and 14.50 m H. Each

deposit is located on the uphill side of and adjacent to a subunit 6a channel margin. The deposits consist of mudstone with varying amounts of angular mudstone clasts; this lithology is identical to some subunits in the Troublesome. Deposits of subunit 6b have subtle bedding planes or limonitic streaks; one of the best-preserved bedding planes is plotted on the trench log in the subunit 6b deposit at 4 m H. The bedding planes are steeper than bedding in underlying Troublesome strata. The deposit of subunit 6b at 4 m H also is underlain by gravelly sand correlated with unit 5. We interpret the three deposits of subunit 6b as blocks of Troublesome Formation. The blocks slumped off the wall of the scarp into the channel where deposition of subunit 6a occurred. Erosion of the top or side of each block of subunit 6b occurred before the deposition of overlying deposits of subunit 6a.

A key question related to the origin of the trenched scarp involves the age or ages of the subunit 6a sediment in the channels. Are all the subunit 6a deposits principally of one age, simply blanketing a pre-existing scarp, or were the sediments deposited during individual random events that "spilled off" the surface above the scarp at a different place during each event? Or is the oldest subunit 6a sediment at the top of the scarp and the youngest at the base, indicating progressive step-down of the channels as if the creation of the scarp occurred over time? If so, then each channel step-down may have formed in response to a sudden upward-folding movement of the bedrock, or to pulses of erosional incision on the lower side of the scarp. We revisit this question later in the Potential Origins section.

Soil Development and Weathering Profile

The only pedogenic soil observed in the trench is a weak soil formed at the top of subunit 6a across the entire length of the trench. No buried paleosols were documented in the trench on units 2 through 5. Before deposition of younger units, episodes of erosion may have removed soils on units 2 through 5, or the time between deposition of these units was short. The deposition of the next youngest unit then occurred before little to no pedogenic soil developed.

The young soil profile that mantles the ground surface across the entire trench consists of an organic (Oi) horizon that varies from about 4 to 18 cm thick, and an underlying, slightly clay-rich A horizon that ranges from about 8 to 40 cm thick (note: pedogenic soil nomenclature is from Birkeland, 1999). Weakly developed C and Cox horizons are found beneath the A horizon; they extend across the entire length of the mapped trench wall and have a combined thickness ranging from about 5 to 55 cm.

In much of the trench, the upper 1 to 1.5 m of the Troublesome Formation is weathered (see **Plate 1**). Unweathered Troublesome strata tend to be blocky, whereas weathered strata lack the blocky character, are less lithified, and have higher clay content. The base of the weathering zone roughly parallels the base of unit 6, and it appears to terminate at ~11 m H. We infer that fractures in bedrock strata probably were more closely spaced in the section of the trench where bedrock strata are anticlinally folded. This occurrence generally coincides with the extent of the weathered zone. The higher number of fractures would allow water to infiltrate into the rock more efficiently and increase weathering rates.

Geochronology

Shannon Mahan, U.S. Geological Survey (USGS), with assistance from Lauren Heerschap (CGS), collected and analyzed five samples for Optically Stimulated Luminescence (OSL) dating. OSL is a geochronological method of determining the age of burial for sediment deposited after recent transportation. Luminescence estimates the time that has elapsed since those minerals in the sediment were exposed to sunlight before burial using trapped electron charges as dosimeters. Once mineral grains of quartz or potassium feldspar rest within the body of the sediment, they are removed from light and are exposed to ionizing radiation from naturally occurring low-level radionuclides of potassium, uranium, and thorium. Cosmic rays provide an outer space component of the ionizing radiation, but its effects are most significant at high elevation and near the ground surface.

This ionizing radiation dislodges electrons from their host atoms, creating ions and free electrons. Point defects capture a fraction of these free electrons before they can "relax" to a ground state, and in this way, the number of trapped electrons increases over time. The system becomes saturated over time as well. Hence, the limit for luminescence dating is highly dependent on source geology (i.e., amount of K, U, and Th elements in local sediment). Exposure to ultraviolet or visible light untraps all previously trapped electrons. This process is called "bleaching" or "zeroing" and occurs along the path of transport (photons from sunlight have sufficient energy to liberate electrons bonded to optical traps but not enough energy to generate new electrons (Brown, 2017). Ideally, the transport path is long enough or varied enough to allow for 5 to 30 minutes of sunlight exposure.

We ran two types of analyses for each sample: Infrared Stimulated Luminescence (IRSL) on feldspars and Blue-Light OSL on quartz. IRSL analyses used silt-sized

(4 to 11-micron size) feldspar grains, and the Blue-Light OSL analyses used fine sand-sized (180 to 250-micron size) quartz grains. Each type of testing required a different type of preparation and analysis protocol, as shown in **Appendix B**. In general, feldspars saturate at a slower rate than quartz. Still, quartz bleaches quicker on the transport path. We expected a few of the samples were quite old (e.g.>200 ka). As such, we used both analyses so that the effects of "partial bleaching" could be tested and mitigated in samples.

Plate 1 shows the locations of the samples on the trench log. Three of the samples were from gravelly sands in subunit 6a. Samples locations are at 3.0 m H and -1.80 m V (WF-OSL-1); 9.18 m H and -3.20 m V (WF-OSL-2); and 14.50 m H and -4.92 m V (WF-OSL-3). Sample WF-OSL-4 was collected from gravelly sandstone in subunit 1b at 12.53 m H and -5.80 mV to test our correlation of this unit with the Troublesome Formation. WF-OSL-5 was collected from subunit 2b at 20.80 m H and -6.90 m V to assess our interpretation that the deposition of this unit occurred during the Late Quaternary. **Table 1** summarizes the results for geochronology dating. See **APPENDIX B** for detailed data and results.

Table 1 – Geochronology results. Preferred ages are in bold. Terms upper, central, and lower parts refer to where on the lower scarp the sample was collected.

Sample	IRSL Feldspar Dates (ka)	OSL Quartz Dates (ka)
WF-OSL-1, **subunit 6a**, upper part of scarp face	28.7 ± 1.40	**10.8 ± 0.56**
WF-OSL-2, **subunit 6a**, central part of scarp face	21.3 ± 1.87	**10.1 ± 0.49**
WF-OSL-3, **subunit 6a**, lower part of scarp face	**12.7 ± 1.46** 18.7 ± 0.98	**12.0 ± 0.53**
WF-OSL-4, **subunit 1b**, central part scarp	No result	No result
WF-OSL-5, **subunit 2b**, base of scarp	**>147 ± 30.9** **>143 ± 37.2**	No result

For samples 1, 2, and 3, all from subunit 6a, different results were obtained for the two dating techniques. The OSL quartz dates for those samples are much younger than the corresponding IRSL feldspar dates. The OSL dates indicate an Early Holocene to latest Pleistocene age for the three samples from subunit 6a. All OSL samples collected in unit 6a are similar in age, considering degree-of-error value.

The feldspar IRSL dates indicate a Late Pleistocene age for the deposit, with the youngest sediment at the lower part of the lower scarp and the oldest sediment at the upper part of the lower scarp. There are two reasonable explanations for the age/stratigraphic disconnect between the OSL and IRSL dates. One is that the upper and middle scarp areas were deposited very quickly under limited-sunlight process transport. The second explanation is that the material contained large amounts of slump-incorporated material not separated in the polymineral analyses of silt-sized feldspars. The second explanation appears to be particularly true for WF-OSL-2, which was collected immediately above subunit 6b, a slump block of Troublesome Formation. Since we know IRSL on feldspars takes longer to zero than OSL on quartz (Gray and others, 2015), this can lead us to a further, focused observation. The material for WF-OSL-3 was better bleached at deposition. Both the quartz and the feldspar ages match within error despite the collection of WF-OSL-3 above a slump block of subunit 6b.

We believe the more reliable dates come from the quartz OSL, in which case the unit 6a deposit is of a similar age, ~10 to ~12 ka, throughout the upper, middle, and lower parts of the scarp face. Thus, unit 6a is Early Holocene in age, or perhaps Latest Pleistocene. However, we cannot rule out that all ages might be maximum ages of scarp development due to some degree of inadequate resetting of previous luminescence signals (Gray and others, 2015). No testing results were obtained for sample WF-OSL-4, collected from unit 1b. The luminescence signal was saturated well beyond our current capability to measure, indicating the sediment is older than the Late Quaternary. While this result does not uniquely identify the unit as being the Miocene/late Oligocene Troublesome Formation, it indicates that it is not a Late Quaternary deposit.

Sample WF-OSL-5, collected in unit 2b, resulted in two saturated results ("greater than" 147 and 143 ka) for IRSL feldspar. These results indicate either a pre-late Middle Pleistocene age for the deposit (such as Bull Lake glaciation; MIS 6) or a sizeable partial bleach bias from incomplete resetting before deposition. We were unable to obtain usable results for the OSL quartz run due to the lack of a dominant fast component for the quartz (Gray and others, 2015). We regard the old feldspar IRSL dates on sample WF-OSL-5 as a result of partial bleaching bias rather than recording a depositional event. Such evidence includes:

1) the stratigraphic and geomorphic position of unit 2 relative to unit 6;

2) the lack of pedogenic soil development on unit 2; and

3) weak weathering of clasts in unit 2,

all of which indicate an age younger than the IRSL results. Additionally, IRSL samples from subunit 6a demonstrably suffered from partial bleaching. Based on this evidence, our pre ferred interpretation is that unit 2 is Late Pleistocene in age.

Structure Exposed In Trench

The trench did not expose fault planes, tilted or folded Quaternary strata, or other definitive evidence of deformation of Quaternary units. The primary structural feature exposed in the trench is folding in the Troublesome bedrock (see Plate 1). In most of the trench, strata in the Troublesome dip north, roughly parallel to the face of the lower scarp. The bedding becomes less steep towards the top and base of the scarp. In the southern part of the trench, bedrock strata roll over and dip south at ~8 m H for lower strata and ~5 m H for upper strata, exposing what appears to be an asymmetrical anticlinal fold in the bedrock or a minor flexure on a monoclinal structure. The structural rollover occurs 1 to 3 m south of the crest of the lower scarp. The limited exposure of the rollover in the trench precludes a conclusive assessment of which structural interpretation is correct, as well as whether the rollover and scarp are genetically related. It is possible that the folding of bedrock predates the Late Quaternary, or the folding resulted from a process other than tectonism, such as landsliding.

Structural attitudes (strike and dip) were measured on Troublesome beds at ten locations within the trench. Eight of the measurements were on the north side of the rollover, and two were on the south side of the rollover. Measured strikes on the north side of the rollover ranged from 84 to 96° (N84°E to S84°E). The mean of the measured strikes on the north side of the rollover is about 85° (N85°E), which is similar to the strike of the scarp at the trench. The strike of bedding on the south side of the rollover is more variable. At the two locations where strike could be measured on the south side of the rollover the strikes were 60° (N60°E) on the subunit 1d/1e contact and 110° (S60°E) on the subunit 1c/1d contact.

Beds on the north side of the rollover consistently dip 20 to 22° north until ~13 m H, then flatten to ~12° north until ~17 m H. From there to the north end of the logged trench bedding was not apparent in the limited exposures of bedrock in that section of the trench. Bedding on the north side of the anticlinal rollover is subparallel to the scarp face, which has a maximum slope angle of 19.5° and average slope angle of about 14°.

We could measure the dip of bedrock on the south side of the rollover at three locations on the east trench wall, with values of 19° SW, 24° SE, and an apparent dip of 16° generally south (strike could not be accurately determined). On the west trench wall, the contact between subunits 1d/1e steepened to an apparent dip of about 45° at the trench floor.

The axial plane of the anticlinal feature is not vertical (Plate 1). At the top of unit 1e, the axis is at about 5.9 m H. At the top of unit 1d, the axis is at about 6.3 m H, and at the top of unit 11c it is at about 7.5 m H. Based on these axial positions, the apparent axial plane of the anticlinal feature dips about 30° south. This is rather flat for a tectonic structure formed in an extensional environment and more typical of compressional tectonism or a landslide sip plane. Compressional tectonism is not known to have affected the region syn- or post-deposition of the Troublesome Formation (e.g., Tweto, 1979; Berglund, 2012), making it unlikely that the fold is a result of compressional tectonism.

Subunits 1c, 1d, and 1e thin northward as they cross the anticlinal axis and extend down the north limb of the fold. For example, unit 1e is about 50 cm thick on the south fold limb but is less than 20 cm thick on the north fold limb. All three subunits consist of mudstone on the south fold limb but contain varying amounts of angular mudstone clasts with a mudstone matrix on the north fold limb. Initially, we interpreted these angular clasts as rip-up clasts, but they also may reflect localized, brittle brecciation of the mudstone strata during deformation.

For this report, we infer the structural feature exposed in bedrock is an anticlinal or antiformal feature and call it the Watt anticlinal fold. Named for the landowner, who not only gave permission for a trench but also excavated and helped to shore it. In this interpretation, the face of the lower scarp approximately parallels north-dipping Troublesome strata in the north limb of the Watt anticlinal fold. An alternate interpretation is that the south-dipping strata are a localized minor flexure on an otherwise overall north-dipping monocline, whose upper part was removed by erosion. The bedrock structure also could be interpreted as deformation associated with an unrecognized landslide, an interpretation that we slightly favor.

As described in the Geologic Setting section, the Williams Fork Mountains fault consists of a series of en echelon traces whose ends often overlap (Kirkham, 2003; Kellogg and others, 2011). One of the previously mapped, right-stepping, en echelon overlap ends at about Copper Creek. Water well drillers logs indicate this section of overlapping en echelon faults extends northward at least to near Johnson Gulch. The well data do not preclude the possibility that the en echelon fault pattern potentially could extend northwest to McQueary Gulch. If the en echelon fault pattern does continue to McQueary Gulch, the lower scarp might be related to the overlapping northern end of an en echelon fault.

POTENTIAL ORIGINS AND AGE OF THE LOWER SCARP

The McQueary Gulch trench did not reveal conclusive evidence of the origin of the lower scarp. Potential origins include Late Quaternary faulting that transitioned upward into a fold in weakly lithified, clay-rich Troublesome strata that extended to the ground surface. Other possible origins include deformation within or at the toe of a landslide, fluvial erosion, soft-sediment deformation or compaction of underlying sediments, and differential erosion of a pre-Quaternary tectonic fold.

Strata in the northern limb of the Watt anticlinal fold are roughly parallel to the face of the lower scarp. This geometry suggests the lower scarp might be related to the bedrock structure. However, the anticlinal rollover in bedrock does not coincide with the crest of the scarp. Instead, the rollover is located upslope of the scarp crest. The subparallel relationship between the dip of Troublesome strata with the face of the scarp may be coincidental. If correct, then the fold may not be the direct cause of the scarp.

Since the upper scarp aligns with the range front, where Proterozoic rocks are in fault contact with Troublesome strata, it probably is at least in part a tectonic feature. However, the upper scarp may also have served as a pre-Late Quaternary landslide headscarp. If correct, this may explain the unusual height of the scarp. The scarp height being a result of tectonic uplift and lowering of the ground surface in the zone of depletion of a landslide (Cruden and Varnes, 1996). The range front and fault-line scarp are concave to the southwest. In contrast, the lower scarp is concave to the northeast and has Troublesome strata on both sides. To the south-southeast, the upper scarp continues to follow the fault-line scarp at the range front. In contrast, the lower scarp appears to terminate in colluvial deposits about 50 m east of the trench. We cannot, with certainty, project the lower scarp to a saddle on a ridge formed in Troublesome strata on the southeast side of McQueary Gulch.

We attribute the highly variable strike orientations of bedding within the Troublesome Formation south/upslope of the anticlinal rollover to thickening and thinning of weakly lithified, clay-rich beds in a local fold. This type of feature could develop in the shallow subsurface in either a tectonic fold or in areas subject to compression within a landslide.

The folding in unit 1 of the Troublesome strata is similar to compression-folding features, particularly transverse ridges, commonly seen within and at the toes of some landslides (Cruden and Varnes, 1996). The lower scarp may be at the toe of an unrecognized landslide. In an alternative landslide scenario, one could associate the lower scarp with a transverse ridge within a larger landslide that occupies the relatively broad, aspen-filled basin downslope of the range front. The broad, aspen-filled basin is unlike other range-front basins elsewhere in the hanging wall of the Williams Fork Mountains fault. The Troublesome Formation is clay rich, weakly consolidated, and known to be landslide prone even where not tectonically deformed (Izett, 1968, 1975; Izett and Barclay, 1973). Also, the lack of resetting seen in the sediments collected for luminescence dating supports a process that involves large and sudden mass movements. Such mass movements are unlike the normal colluvial processes for which luminescence dating has been well documented and relied upon (Gray and others, 2015).

Dating of sediment that drapes the lower scarp (subunit 6a) or is incised against its lower end (unit 2) suggests the anticlinal fold in the Troublesome Formation, regardless of its origin, almost certainly occurred during or before the Late Pleistocene. The luminescence ages indicate the last depositional events on the scarp (unit 6) are no younger than ~9 ka (at 2 sigma error). Unit 2 alluvial fan deposits bypass and wrap around the base of the lower scarp. This suggests the full formation of the scarp occurred before the deposition of unit 2. If correct, the lower scarp formed before late Middle Pleistocene time, based on OSL ages of >147 ± 31 and >143 ± 37 ka on unit 2, or perhaps during the Late Pleistocene if the dated samples were not completely reset before burial and only partially bleached when deposited. Additional evidence supporting a Late Pleistocene age for unit 2 includes the stratigraphic and geomorphic position of unit 2 relative to unit 6, the lack of pedogenic soil development on unit 2, and weak weathering of clasts in unit 2. All of which indicate an age younger than the OSL results (see Appendix B and Geochronology section).

If the lower scarp existed before, or coincident with, deposition of unit 2, then units 3, 4, 5, and 6 are all associated with modifications of the existing scarp face. Units 3, 4, and 5 probably are a result of slumping or erosion of the scarp face. Unit 6, a latest Pleistocene to Early Holocene deposit with alluvial affinities, overlies the entire scarp. It probably formed from debris flows or hyperconcentrated flows spreading across the bench upslope from the scarp crest and spilling over and locally eroding the scarp face. Little evidence of stratification in unit 6 remains. The lack of preservation of stratification precludes the assessment of whether the scarp grew since the deposition of unit 6.

As for the nature and timing of the deposition of subunit 6a, luminescence dating results point to two different scenarios:

1) The IRSL dating (of feldspar silt) suggests either that the draping 6a deposits become younger toward the base of the scarp, over a period of at least 10 to 16

ky (thousand years) during the Late Pleistocene; or that the deposition of unit 6 began subtly and slowly because the lower part of the unit is well bleached but then ended in mass-wasting processes because the upper and middle parts of the unit contain large partial bleaching bias in the luminescence ages that were recorded.

2) Conversely, the blue-light OSL dating (of quartz) shows a random scatter down the trench face, which can be interpreted either as deposition over a period of about 2 ky during the Late Pleistocene to Early Holocene transition or during the same time period in short indistinguishable depositional processes.

Although the evidence is not conclusive, our preferred interpretation is that both the scarp and anticlinal fold in bedrock are a result of slope instability. The scarp formed at the toe of a landslide or at the toe of a transverse ridge within a landslide whose headscarp probably coincided with the upper scarp. After the landslide formed, surface water flowing along the base of the landslide scarp deposited unit 2. Whether the scarp was wholly or partially buried by sediment after deposition of unit 2 is uncertain. Still, the absence of any pedogenic soil on unit 2, its irregularly eroded upper surface, and the lack of weathered clasts within it, suggest unit 2 is a basal remnant of a once thicker deposit. Based on OSL dates within unit 2, the lower scarp and inferred landslide developed during or before Late Pleistocene time. Geomorphic evidence of the inferred landslide may be obscured by subsequent erosional and depositional events before or during the deposition of unit 6.

We considered, but discarded, other potential origins for the scarp and bedrock fold because available data did not support them. Alternatives considered include Late Quaternary tectonic folding, fluvial erosion, differential compaction of underlying sediments, and erosional modification of a pre-Quaternary tectonic fold. For example, tectonic folding of ductile Troublesome strata that propagated upwards from brittle faulting at depth, or that the fold formed in the hanging wall of the fault strand at the range front are not viable interpretations. They are not viable because the anticlinal fold does not coincide with the top of the scarp, nor is it downslope of the top of the scarp as would be the case if the scarp had retreated since formation. Admittedly, due to the limited exposure of the rollover and south-dipping beds, one could attribute the anticlinal rollover to a localized minor feature on an overall monoclinal fold. However, the lower scarp also is concave in plan view, in the opposite direction of the range front. Furthermore, the lower scarp cannot be traced laterally beyond the basin floor of McQueary Gulch. These factors also suggest an origin other than recent tectonism.

It is unlikely that fluvial erosion carved the lower scarp because most streams that drain the east flank of the Williams Fork Mountain align nearly perpendicular to the range front, not at a sharp oblique angle to it. If differential compaction caused the scarp, similar scarps, and other deformational features typical of differential compaction should exist along the range front in nearby areas. However, we could not find evidence of such features.

Soft sediment deformation due to compaction of underlying sediments is an unlikely cause of the fold and scarp. Such processes typically occur relatively soon after sediment deposition, which was during the late Oligocene-Miocene. Yet, the scarp persists as a prominent geomorphic feature even though it is in weakly lithified, easily eroded bedrock strata. Erosion and exhumation of a pre-Quaternary tectonic fold also is unlikely, because when exhumed, the easily eroded strata in the fold would tend to be beveled, and not result in a scarp when subjected to erosion at the ground surface.

SUMMARY

In 2005 the Colorado Geological Survey conducted a paleoseismic investigation in McQueary Gulch at the northern end of the Williams Fork Mountains fault. The fault is a normal fault along the west side of the Williams Fork Valley, one of the northernmost basins within the Rio Grande rift. Although this location was not optimal for a paleoseismic investigation, it was the best location for a trench given budgetary, access, and scheduling constraints.

The main trace of the Williams Fork Mountains fault is at the range front, where Proterozoic crystalline rocks are in fault contact with the Miocene and late Oligocene Troublesome Formation, which comprises all syn-rift sediment in this rift basin. A prominent scarp in surficial deposits aligns with the fault-line scarp at the range front. Known as the upper scarp, it is 10.8 m high, has a maximum scarp angle of 19.5°, and an apparent surface offset of 5.8 m (Kirkham, 2003). A paleoseismic trench across such a tall scarp would require a large trench, which was far beyond the scope and budget of our project. A secondary scarp, called the lower scarp, is located in the hanging wall of the main fault trace about 50 to 80 m north-northeast of and downslope of the upper scarp at the range front. The lower scarp is 4.8 m high and has a maximum scarp angle of 22.0°.

A single slot trench was excavated across the lower, secondary scarp and studied during the investigation. A significant volume of groundwater flowed into the trench, creating stability issues for trench walls. One section of the trench wall failed during the first night after trench excavation, even though the contractor installed shores to reduce the likeli-

hood of wall failures. The next day the trench was extended ~27 m downslope to allow groundwater entering the trench to discharge onto the ground surface. We logged only the shored upper 23 m of the east trench wall.

Six major stratigraphic units and 15 minor subunits were identified based on lithologic properties and relative ages. The oldest unit exposed in the trench (unit 1) is the Miocene and late Oligocene Troublesome Formation, which consists mostly of mudstone and mud-clast mudstone in the trench. Unit 2 is the oldest Quaternary deposit exposed in the trench. This alluvial unit occurs at the base of the lower scarp in what appears to be a channel that may wrap around the scarp. Our preferred interpretation is that the scarp formed before the deposition of unit 2. After formation, multiple periods of erosion and deposition altered the scarp. IRSL feldspar dating of samples from unit 2b yielded saturated results of >147 ± 31 ka and >143 ± 37 ka. We believe these ages result from a significant partial bleach bias due to incomplete resetting before deposition. As such, we conclude unit 2 probably is Late Pleistocene, not pre-late Middle Pleistocene, as indicated by the IRSL dating.

Units 3, 4, and 5 are interpreted as slump blocks locally derived from bedrock exposed on the scarp face or as colluvium or mud flows deposited on the scarp face. We did not obtain absolute ages for these three units. Relative dating indicates these units are younger than Late Pleistocene unit 2 and older than overlying Holocene or latest Pleistocene unit 6, which is alluvium that drapes the scarp face. We interpret units 3,4 and 5 as Early Holocene or perhaps latest Pleistocene based on OSL dating.

The authors saw no definitive evidence of Late Quaternary faulting or folding in the trench. The most impressive structural feature in the trench is a long section of north-dipping Troublesome strata that is subparallel to the face of the lower scarp. The strata then rolls over into an anticlinal fold near the top of the scarp in the upper/southern end of the trench. The trench wall exposed only a few meters of south-dipping beds in the southern limb of the anticline. The anticlinal rollover could be a minor feature on a larger monoclinal fold related to deformation in the hanging wall of the main fault trace at the range front. However, we assume the rollover is the crest of an anticline or antiformal feature that we call the Watt anticlinal fold.

Folding is not commonly associated with extensional tectonics. Still, the brittle deformation associated with a normal fault at depth could transition upward into a fold or a complexly folded structure when passing through thick strata like the Troublesome Formation, with its weakly lithified sedimentary deposits that can deform plastically, especially when saturated. The subparallel relationship between the scarp face and the north-dipping strata in the northern limb of the anticlinal fold suggests the fold may have played a role in the formation of the scarp.

In plan view, the Williams Fork Mountains fault consists of a series of fault strands whose ends tend to overlap with adjacent strands, often in a right-stepping pattern. Mapping by Kirkham (2003) and Kellogg and others (2011) shows overlapping fault strands in the Johnson Gulch-Copper Creek area, immediately south of McQueary Gulch. Water-well data described in the Geologic Setting section supports this interpretation. Grauch and others (2013) and Watkins (1996) documented an outbound fault locally in the hanging wall of the Sangre de Cristo fault, the master fault in the San Luis Basin.

If overlapping fault strands or an outbound subparallel fault existed in the McQueary Gulch area, the trenched lower scarp might be related to such a fault. Still, there is no definitive evidence that an overlapping or subparallel fault strand is present in McQueary Gulch, especially at the location of the lower scarp.

Given available data, our preferred interpretation is that the scarp and fold formed at the toe of an unrecognized landslide, or at a transverse ridge within a landslide during or before the Late Pleistocene. The headscarp of the landslide probably coincides with the upper scarp. Geomorphic evidence of the landslide between the upper and lower scarps, if it once existed, probably was obscured by subsequent erosional and depositional events before deposition of unit 6 (unit Qa2 shown on Figure 6).

Although the McQueary Gulch trench did not yield direct evidence of Late Quaternary activity on the Williams Fork Mountain fault, prior studies by Unruh and others (1993; 1996), Kirkham (2003), and Kirkham and Lindsay (2003) indicate that paleoseismic studies at more favorable locations along the fault, such as at the Middle Mule Creek or Lost Creek sites, are warranted. Additionally, a more extensive trench on the upper scarp at the range front in McQueary Gulch could yield paleoseismic evidence of Late Quaternary faulting. However, interpretation could be complex if the upper scarp also served as a landslide headscarp.

ACKNOWLEDGEMENTS

We thank Milton Watt for allowing CGS to dig the trench on his property. Mr. Watt also excavated and backfilled the trench for us. He and his daughter Becky provided essential assistance that allowed for the successful installation of the shoring system and the dewatering of the trench. We also thank Tony Crone and Mike Machette, USGS, for loaning the shores to us. Thoughtful peer review comments by Dean Ostenaa, Kevin McCoy, and Karen Berry significantly improved the report. Larry Scott prepared the report layout and figures 1 and 3.

REFERENCES CITED

Berglund, H.T., Sheehan, A.F., Murray, M.H., Roy, M., Lowry, A.R., Nerem, R.S., and Blume, F., 2012, Distributed deformation across the Rio Grande rift, Great Plains, and Colorado Plateau: Geology, v. 40, no. 1, p. 23–26.

Birkeland, P.W., 1999, Soils and geomorphology: Oxford University Press, 3rd edition, 430 p.

Brown, N.B., 2017, Using luminescence signals from bedrock feldspars for low-temperature thermochronology: Ph.D. Dissertation, University of California, Los Angeles.

Cruden, D.M., and Varnes, D.J., 1996, Landslide types and processes, in Turner, A.K., and Schuster, eds., Landslides – Investigation and Mitigation: Washington, D.C., National Academy Press, Transportation Research Board, National Research Council, Chapter Three, p. 36–76.

Gray, H. J., Mahan, S. A., Rittenour, T., and Nelson, M., 2015, Guide to luminescence dating techniques and their applications for paleoseismic research, invited paper in Lund, W.R., editor, Proceedings volume, Basin and Range Province Seismic Hazards Summit III (BRPSHSIII): Utah Geological Survey Miscellaneous Publication 15-30, variously paginated.

Grauch, V.J.S., Bedrosian, P.A., and Drenth, B.J., 2013, Advancements in understanding the aeromagnetic expressions of basin-margin faults--An example from San Luis Basin, Colorado: Society of Exploration Geophysicists, The Leading Edge, v. 32, no. 8, p. 882–891.

Izett, G.A., 1968, Geology of the Hot Sulphur Springs quadrangle, Grand County, Colorado: U.S. Geological Survey Professional Paper 586, 79 p.

Izett, G.A., 1975, Late Cenozoic sedimentation and deformation in northern Colorado and adjoining areas, in Curtis, B.F., ed., Cenozoic history of the southern Rocky Mountains: Geological Society of America, Memoir 144, p. 179–209.

Izett, G.A., and Barclay, C.S., 1973, Geologic map of the Kremmling quadrangle, Grand County, Colorado: U.S. Geological Survey Geologic Quadrangle map GQ-1115, scale 1:62,500.

Izett, G.A., and Obradovich, J.D., 2001, 40Ar/39Ar ages of Miocene tuffs in basin-fill deposits (Santa Fe Group, New Mexico, and Troublesome Formation, Colorado) of the Rio Grande rift system: The Mountain Geologist, v. 38, no. 2, p. 77–86.

Kellogg, K.S., 1999, Neogene basins of the northern Rio Grande rift--Partitioning and asymmetry inherited from Laramide and older uplifts: Tectonophysics, v. 305, p. 141–152.

Kellogg, K.S., Shroba, R.R., Premo, W.R., and Bryant, Bruce, 2011, Geologic map of the eastern half of the Vail 30' x 60' quadrangle, Eagle, Summit, and Grand Counties, Colorado: U.S. Geological Survey Scientific Investigations Map 3170, scale 1:100,000, 49 p. pamphlet.

Kirkham, R.M., 2003, Quaternary faulting in the Williams Fork Valley graben, north-central Colorado, and comparison with late Quaternary deformation near Spinney Mountain, central Colorado: Colorado Geological Survey report submitted as deliverable for National Earthquake Hazard Reduction Program External Grant Award 02HQGR0102, 46 p., available on the USGS website.

Kirkham, R.M., and Lindsay, N.R., 2003, Williams Fork Valley graben: The northernmost documented late Quaternary structure in the Rio Grande rift system [abs.]: Geological Society of America Abstracts with Programs, v. 35, no. 5, p. 15.

Lovering, T.S., 1930, The Granby anticline, Grand County, Colorado: U.S. Geological Survey Bulletin 822-B, p. 71–76.

Shroba, R.R., Bryant, Bruce, Kellogg, K.S., Theobald, P.K., and Brandt, T.R., 2010, Geologic map of the Fraser quadrangle, Grand County, Colorado: U.S. Geological Survey Scientific Investigations Map 3130, scale 1:24,000, 26 p. pamphlet.

Tweto, Ogden, 1973, Reconnaissance geologic map of the Mount Powell 15- minute quadrangle, Grand, Summit, and Eagle Counties, Colorado: U.S. Geological Survey Open-File Report 73-286, scale 1:62,500.

Tweto, Ogden, 1978, Tectonic map of the Rio Grande rift system in Colorado, in Hawley, J.W., compiler, Guidebook to Rio Grande rift in New Mexico and Colorado: New Mexico Bureau of Mines and Mineral Resources Circular 163, scale 1:1,000,000.

Tweto, Ogden, 1979, The Rio Grande rift system in Colorado, in Riecker, R.E., ed., Rio Grande rift: Tectonics and magmatism: American Geophysical Union, p. 33–56.

Tweto, Ogden, Moench, R.H., and Reed, J.C., 1978, Geologic map of the Leadville 1° x 2° quadrangle, northwestern Colorado: U.S. Geological Survey Miscellaneous Geologic Investigations I-999, scale 1:250,00.

Tweto, Ogden, and Reed, J.C., Jr., 1973, Reconnaissance geologic map of the Ute Peak 15-minute quadrangle, Grand and Summit Counties, Colorado: U.S. Geological Survey Open-File Report 73-288, scale 1:62,500.

Unruh, J.R., Wong, I.G., Bott, J.D.J., Silva, W.J., and Lettis, W.R., 1993, Seismotectonic evaluation, Rifle Gap dam-Silt project, Ruedi dam-Fryingpan-Arkansas project: report prepared by

William Lettis & Associates for U.S. Bureau of Reclamation, 154 p.

Unruh, J.R., Sawyer, T., Lettis, W.R., 1996, Draft report-Seismotectonic evaluation-Granby, Green Mountain, Shadow Mountain, and Willow Creek Dams, Colorado-Big Thompson Project: prepared by William Lettis & Associates, Inc., Walnut Creek, California for U.S. Bureau of Reclamation, Denver, Colorado, 77 p.

Watkins, T.A., 1996, Geology of the northeastern San Luis Basin, Saguache County, Colorado, in Thompson, R.A., Hudson, M.R., and Pilmore, C.L., eds., Geologic excursions to the Rocky Mountains and beyond; Field trip guidebook for the 1996 annual meeting: Geological Society of America Special Publication 44 and Colorado Geological Survey CD-ROM.

APPENDIX A. UNIT DESCRIPTIONS

Unit 1 -- Miocene and late Oligocene Troublesome Formation:

Subunit 1a is the lowest and oldest subunit in the trench. We traced it from 8 m H to 22 m H. Unit 1a consists of brown (7.5 YR 4/4) and reddish-yellow (7.5 YR 6/6) claystone that is slightly silty and sandy. The claystone is smectitic and contains a trace of mica. Sand grains range from very fine to fine. The major seep in the trench issues from unit 1a, and the unit is moist to wet. The internal structure of subunit 1a is difficult to discern due to the wetness, but it is generally massive. The lower part of the subunit is blocky, with angular clasts of clay that are 2 to 5 cm in diameter and have the same texture as the surrounding clayey matrix. Smaller diameter clay clasts (<1 cm) are locally present in the upper part of the unit. A few, discontinuous organic laminae indicate internal bedding is parallel to overlying subunit 1b.

Subunit 1b consists of a lens of gravelly sediment that extends from 8.0 m H, where it abruptly terminates against mudstones of the Troublesome Formation, to 17.0 m H, where it is cut out by a younger channel (unit 2). Subunit 1b ranges from about 10 to 40 cm thick. It becomes finer grained and generally thickens from south to north in the trench. In the upper or southern part of the trench, around 9 to 10 m H, the subunit consists of micaceous, poorly sorted, clast-supported, sandy pebble and small cobble gravel. The clasts are angular and composed mostly of Proterozoic intrusive and perhaps metamorphic lithologies. Near 12 m H the unit is a gravelly sand with a gravel content of about 10%. Clay rip-up clasts are present in the unit, and clay-draped foreset beds were noted on the west (unlogged) wall of the trench. The contact with underlying subunit 1a is sharp. Near 9 m H, the basal contact may be erosional. We interpret this subunit to be fluvial in origin.

Subunit 1c is mostly silty claystone with minor amounts of very fine sand. Near 7.50 m H, most of unit 1c consists of hackly mudstone with somewhat chaotic rotated angular clasts and a clayey matrix. The hackly mudstone has a pink, 7.5 YR 7/4 color and contains scattered, dark-brown, 1 mm diameter blebs that locally have limonitic coatings. The top of the hackly mudstone crosscuts bedding within subunits 1c through 1f. The hackly mudstone may mark the base of a weathering zone that formed prior to deposition of unit 6 and before erosion modified the lower part of the scarp. To the north (i.e., down the scarp), the hackly fractures die out and the unit becomes a very silty claystone and clayey siltstone that contains angular pebbles of claystone and siltstone that are similar to the hackly mudstone. The clasts are typically <1 cm in diameter and are pink (7.5 YR 7/4). The matrix is brown (7.5 YR 5/4). The bedding laminations internally look like they are low-angle, slightly wavy cross beds that suggest a flow direction to the north. The upper boundary of the subunit includes a 1 to 2 cm-thick limonitic silt stringer that is interpreted as a bed with sharp depositional contacts. At about 13.60 m H, and to the north, the limonitic silt stringer at the top of subunit 1c dies out. Since the beds above and below the limonitic silt stringer are similar, it is not possible to discern a contact between them north of where the stringer ends.

Subunit 1d consists of two facies that are similar to the two facies in subunit 1c. Near and south of the crest of the fold, it is chiefly a hackly mudstone. A mudstone with angular claystone and siltstone clasts as much as 1 cm in diameter overlies and is north of the hackly mudstone. The contact between the facies is interpreted to be a weathering contact, as it appears to cut across bedding planes. A limonitic silt or very fine sand bed marks the top of the subunit. The limonitic bed extends from 5.20 m H to 7.80 m H. Beyond the lateral limits of the limonitic bed, subunit 1d cannot be differentiated from either overlying or underlying subunits.

Subunit 1e Subunit 1e is the highest, light-brown (ashy?) subunit in the trench. It is similar to subunits 1c and 1d in that it is composed of two facies, a hackly mudstone facies that occurs at and south of the anticlinal flexure, and a mudstone with sparse mudstone clasts that overlies or is north of the hackly mudstone. The authors interpret the contact between the facies as a weathering contact. Subunit 1e ranges from pink (7.5 YR 7/4) to reddish-yellow (7.5 YR 6/8), and the color is not facies specific. Defining the top of the subunit is a limonitic bed traced from 5.00 m H to 9.20 m H.

Subunit 1f is a mixed deposit of mudstone and mud-clast-bearing mudstone, but the boundaries between two lithologies are gradational and cannot be mapped. On the south side of the crest of the anticlinal fold, the basal part of the subunit is a mud-clast mudstone that grades upward to a mudstone with fewer angular mud clasts. At and immediately north of the anticlinal crest there are poorly defined, wavy ripple and foreset-like laminations that indicate a north current direction. The laminations are moderately steep and some are deformed. As measured along the subunit 1e/1f contact, the laminations have an apparent dip of 22° N on the northern flank of the fold, and 18° S on the back-tilted southern flank. Mud clasts are present in subunit 1f in this part of the trench. Further north, mud clasts are more abundant, and the bedding features die out.

From about 13.60 m H northward to the margin of the unit 2c channel at ~17 m H, subunits 1c through 1f are

mapped as a single subunit (subunit 1f), because the limonitic beds used to differentiate them are not present. In this lower part of the trench, the combined subunits are a mud-clast mudstone with random limonitic staining. The clasts are light-yellowish-brown (10 YR 6/4) and the matrix is mottled brown (7.5 YR 4/4) to reddish-yellow (7.5 YR 6/8).

Subunit 1g is a mud-clast mudstone in which the clasts are more abundant than in the underlying subunit 1f. The clasts in subunit 1g are subangular and mostly <1 cm in diameter. We did not observe bedding in this subunit, which lies on an erosion surface cut into subunit 1f.

Units 2 through 6 -- Quaternary surficial deposits:

Unit 2 is the oldest Quaternary unit exposed in the trench. At the base of the trenched scarp, we observed unit 2 deposited in a channel cut into unit 1. Unit 2 probably was deposited during the Late Quaternary as stream alluvium and debris flows on the fan that underlies the modern drainage to the west and north of the trenched scarp. This fan bypasses the western edge of the scarp and sweeps around the toe of the scarp. We identified three subunits in unit 2. In ascending order, they are subunit 2a, 2b, and 2c. All three onlap onto the channel margin cut into the Troublesome Formation between 17 m H and 19 m H. Subunits 2a and 2b thin towards and pinch out against the channel margin. The preserved, basal part of subunit 2c also terminates at the channel margin. Erosion associated with the unconformity at the base of subunit 6 removed the upper beds in subunit 2c. All three subunits contain varying amounts of gravel composed of Proterozoic lithologies. As described in the GEOCHRONOLOGY section of this report, age-limited OSL dates of older than 147 to 143 ka were measured from unit 2 (subunit 2b) using ISRL dating, indicating that the unit is Middle Pleistocene in age. We regard this result as being erroneous because the stratigraphic and geomorphic position and lack of weathering all indicate a younger age. Based on its position relative to, and beneath, unit 6, it appears that the unit 2 deposit is Late Pleistocene in age.

Subunit 2a is a clast-supported alluvial deposit that coarsens northward. The clasts are subangular to subround. Between 18 m H and 18.60 m H, the subunit consists of sandy pebble gravel, about 10 cm thick. At 22 m H, the subunit thickens to about 50 cm. At 26 m H (in the northward, uncleaned extension of the trench, not shown in the Plate 1 trench log), subunit 2a is at least 1 m thick and consists of sandy cobble gravel. This suggests the base of the subunit 2 channel is cut deeper into unit 1 between 22 and 26 m H. North of 23 m H, subunit 2a contains clast-supported cobble gravel bars. The sand in subunit 2a is dark yellowish-brown (10 YR 4/4). The authors found an unweathered cobble of light-gray to white banded chert in the excavation spoil piles. This clast probably came from subunit 2a around 30 m H.

Subunit 2b is a matrix-supported, slightly gravelly, fine to medium sand that is silty and clayey and has angular clasts. We interpret the subunit as a debris-flow deposit. The sand matrix is dark yellowish brown (10 YR 4/4) and consists of quartz, heavy minerals, mica, and clay.

Subunit 2c is chiefly sandy clay and pebbly clay with angular clasts, probably deposited as a mudflow. The clay is micaceous, yellowish-brown (10 YR 5/4), and lacks bedding. The high clay content indicates that the Troublesome Formation was probably a primary, localized source for the sediment within the subunit.

Unit 3:

A single deposit of unit 3 was encountered in the trench between 16.30 m H and 17.70 m H, on the margin of the channel in which unit 2 was deposited. This block of mud-clast mudstone is lithologically similar to beds within the Troublesome Formation (unit 1). It ranges from pink (7.5 YR 7/4) to reddish-yellow (7.5 YR 7/8). The mud clasts are as much as 3 cm in diameter. Limonitic-stained beds within the block (the most prominent one is shown on the log) indicate it is structurally discordant with the adjacent, in-place Troublesome bedrock. Unit 3 is interpreted as a block of Troublesome Formation that broke loose from the unit 2 channel margin and slumped into the channel over unit 2c. An erosion surface was cut into unit 3 prior to deposition of overlying unit 4.

Unit 4:

A single deposit of unit 4 overlies unit 3. It is a micaceous, sandy, silty clay with scattered, angular, small pebbles composed of Proterozoic lithologies and mudstone. The matrix of unit 4 is brown (7.5 YR 5/4). Numerous irregular limonite stains occur in unit 4. We interpret this unit as either a locally derived mudflow deposit or colluvium. Erosion of the top of unit 4 occurred before the deposition of overlying unit 5.

Unit 5:

The trench exposed five isolated deposits of unit 5. All are micaceous silty clays with varying amounts of widely scattered, angular to subangular pebbles and cobbles composed of Proterozoic lithologies. Since the mud in unit 5 is very similar to that in the Troublesome Formation, we used the presence of gravel clasts to define the contact between unit 5 and the underlying Troublesome bedrock. The gravel clasts are typically <10 cm in diameter. A relatively large deposit of unit 5 occurs between 15 m H and 20 m H. The deposit rests on an erosion surface cut into units 1f, 2c, 3, and 4. In this deposit, gravel casts are larger, attaining diameter as much as 30 cm in

an internal channel at 19.20 m H. Four small deposits of unit 5 occur on the south side of channel step-downs in unit 6 at 4 m H, 11 m H, 12.50 m H, and 14 m H. The four deposits overlie an erosional surface cut into unit 1f. Unit 5 probably was deposited as one or more mudflows or as colluvium; the high mud content indicates the Troublesome Formation was a primary, localized source of the sediment. Since an erosion surface (or surfaces) overlies and separates all five of the isolated deposits, it is uncertain whether they were once part of a single deposit or if they represent multiple episodes of erosion and deposition. The base of each deposit is progressively higher than the next deposit to the north, which suggests the deposits may be colluvium eroded from the face of the scarp.

Unit 6:

Unit 6 is the youngest deposit in the trench. We subdivided it into two subunits.

Subunit 6a, which constitutes nearly all of the unit 6 sediment exposed in the trench wall, consists of gravelly sand and lesser amounts minor sandy gravel with occasional discrete mud drapes. The deposition of the subunit probably occurred as a series of amalgamated hyperconcentrated flood deposits. The gravel clasts in subunit 6a range in size from granules to large cobbles and are composed nearly entirely of subangular Proterozoic lithologies. We observed a single thin, sharp-edged flake of banded chert in subunit 6a at 14.10 m H). The subunit contains poorly sorted sediments, which makes discerning bedding difficult. Small clast-supported bars are locally present, but we could not trace them more than a meter. We also noted a few discrete mud drapes in some channels; the color of the mud was similar to that in the Troublesome Formation.

Subunit 6a forms a continuous sequence of channels that underlie the ground surface across the entire length of the logged trench. The channeled base of unit 6 rests on an unconformity cut into all underlying units. The channels progressively step-down in elevation across the scarp. CGS quickly recognized channel thalwegs and margins where the underlying units are mudstones or gravelly clays. The southern margin of most channels is steeper than the northern margin. Channel thalwegs and margins were impossible to discern internally within the subunit, where similar lithologies are present both in the channel and adjacent or subjacent to it. From the top of the scarp to 14.50 m H, the channels are visible on both trench walls. Measured orientations of the channel thalwegs, margins, and edges suggest the channels in this part of the trench obliquely crossed the scarp (azimuths ranged from 62 to 74°; dips varied from 5 to 10° NE).

In the lower part of the trench, from 14.50 m H to end of the logged trench, exposed channel features in subunit 6a, on the east wall of the trench, do not correlate with similar channel features on the west wall. In the lower part of the trench, deposition of subunit 6a sediments may have occurred in channels that flowed down the scarp, not obliquely across it. The floor of the modern drainage is at the same elevation as the land surface above the scarp, which supports this interpretation.

Subunit 6b: There are three discrete deposits of subunit 6b in the trench at 4 m H, 9 m H, and 14.50 m H. The location of three deposits is on the uphill side of and adjacent to a subunit 6a channel margin. These deposits consist of mudstone with varying amounts of angular mudstone clasts; this lithology is identical to some units in the Troublesome. Deposits of subunit 6b have subtle bedding planes or limonitic-streaks. One of the best-preserved bedding planes is denoted on the trench log in the subunit 6b deposit at 4 m H. The bedding planes are back-rotated relative to bedding in the adjacent Troublesome Formation. The deposit of subunit 6b at 4 m H also is underlain by gravelly sand that appears to be part of unit 5. We interpret the three deposits of subunit 6b as blocks of Troublesome Formation that slumped off the wall of the channel where deposition of subunit 6a occurred. Erosion of the top or side of each block of subunit 6b occurred before the deposition of overlying deposits of subunit 6.

APPENDIX B. OSL DATING RESULTS

By Shannon Mahan, USGS

Radial plots (**Figures 1, 2, and 3 in Appendix B**) are frequently used in luminescence dating to arrive at the most appropriate model of equivalent doses (D_E; the luminescence accumulated in a mineral grain at time of collection), and they have many useful features:

1) D_E values can be viewed simultaneously with their precision of error

2) Automatic sorting of data so that users can easily distinguish D_E estimates in terms of their relative precisions

3) Overdispersion (scatter) can be identified at a glance

4) Recognition of patterns in the data, such as the existence of multiple and discrete D_E components, before calculation of sample age

In general, we recommend that researchers routinely look at radial plots when calculating age models for luminescence. Readers can find more details in Galbraith and Roberts (2012). Not all sample protocols are suited to radial plots. We calculated feldspar using the polymineral grains in a multiple aliquot additive dose protocol. This method is not suitable for radial plots. Therefore, the plots only show quartz.

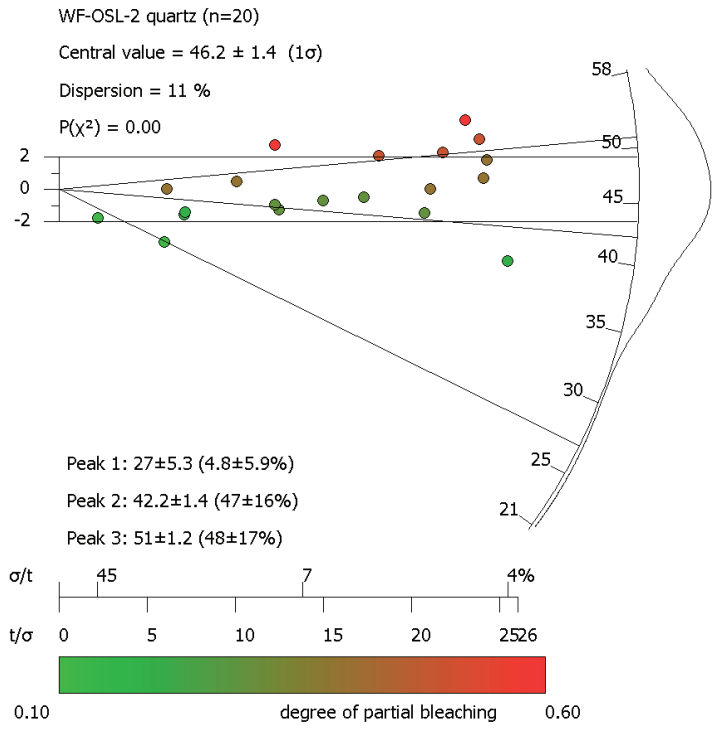

Figure 2 Appendix B – Radial Plot model for sample WF-OSL-2.

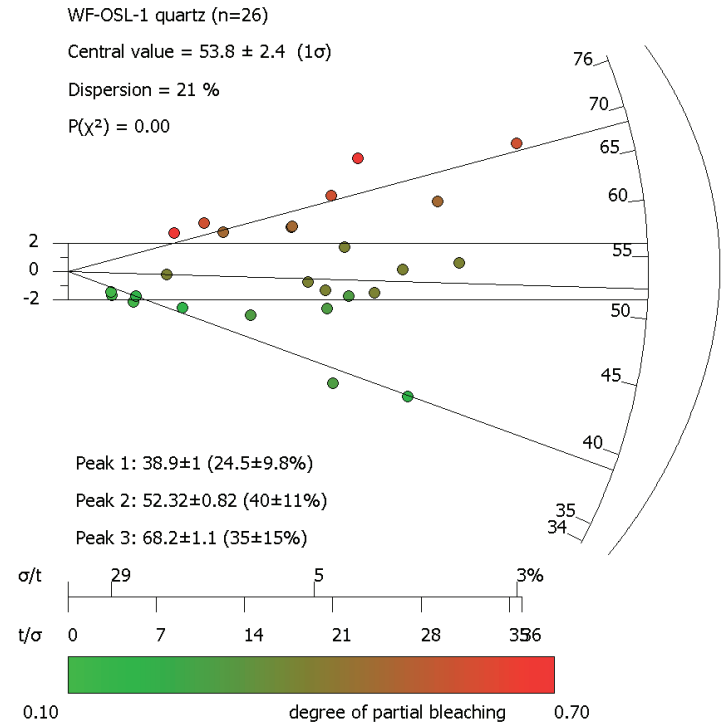

Figure 1 Appendix B – Radial Plot model for sample WF-OSL-1.

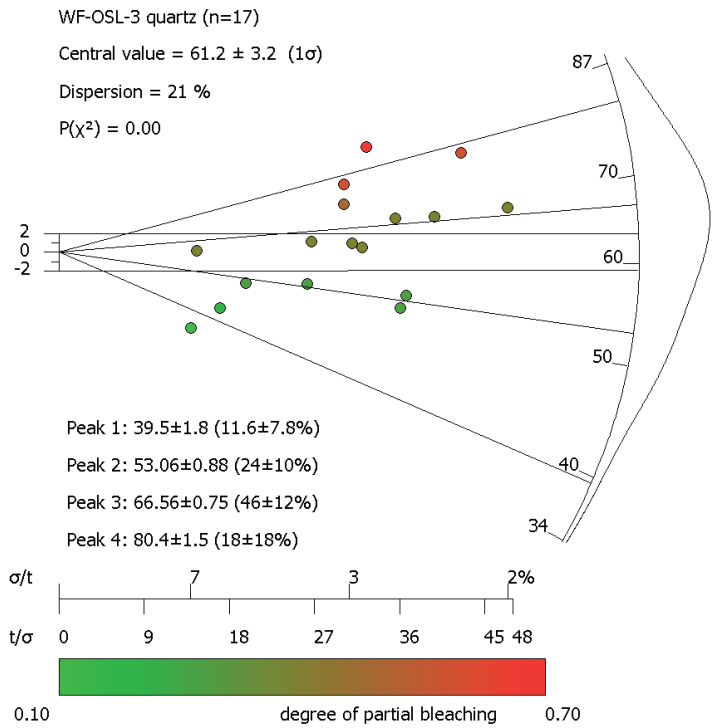

Figure 3 Appendix B – Radial Plot model for sample WF-OSL-3.

QUARTZ

We used Blue-light OSL was done on fine sand-size quartz separates using single aliquot regeneration (SAR) protocols (see **Table 1**). Light stimulation of the quartz was achieved using a RISØ TL-DA-15 reader with an array of blue LEDs centered at 470 nm (15 MW/cm^2). Detection optics were comprised of Hoya 2×U340 and Schott BG-39 filters coupled to an EMI 9635 QA Photomultiplier tube. β radiation was applied using a 25 mCi ^{90}Sr/^{90}Y in-built source (see Table 3 for summary details). The main SAR parameters included use of the 40 second blue-diode wash step of Murray and Wintle (2003) at the same temperature as the preheat temperature and the preferred component of SAR dating (i.e. the 'fast' component, e.g., Murray and Wintle, 2000; Wintle and Murray, 2006; Rhodes, 2011), a signal usually released in the first 0.8 seconds of a typical blue diode stimulation. SAR was used because a dating precision of ~ 10% (sometimes better) can be attained routinely with multigrain SAR quartz methods (e.g., Murray and Olley, 2002) when applied to eolian sand. With SAR, each aliquot yields a distinct D_E value, and thus a distinct age estimate.

POTASSIUM FELDSPARS

Infra-red OSL (IRSL, using infra-red stimulation of potassium feldspars) was done on a polymineralic fine silt fraction (4-11 μm) of potassium feldspars (see **Table 2**). Preheating of silt occurred using an extended, slow temperature of 124°C for 64 hours. IRSL analyses were performed on a Daybreak 1100 luminescence reader with Schott BG-39 filters coupled to an EMI 9635 QA Photomultiplier tube. The silt was dated using the total-bleach multiple-aliquot additive-dose (MAAD) method *(Singhvi and others, 1982; Lang, 1994; Richardson and others, 1997; Forman and Pierson, 2002)*. A minimum of two analyses per IRSL sample by MAAD methods was performed. Anomalous fading tests on the stability of the luminescence signal indicated little to no signal instability (recording ratios of 0.93 to 1.03 for a fade ratio of only 1 to 2 percent). Growth curve data was fit to an exponential trend. All samples were analyzed using continuous wave (CW-OSL) stimulation. The sample size for the silt-sized particles was on the order of many thousands of grains (but no actual count was attempted), covering the entire disc surface.

Table 1 Appendix B. Luminescence parameters used in preparation and analyses of samples for quartz OSL.

Measurement parameters	
Machine	Automated Risø TL/luminescence-DA-15
Mineral; grain size:	quartz: 250-180 microns
Stimulation source:	blue LED diodes, emission centered on 470 nm
Power delivered to aliquot:	14 mW/cm^2 (90% power)
Duration of stimulation:	40 seconds
Final signal level:	4% of initial
Photomultiplier:	Thorn-EMI 9235Q
Aliquot temperature:	125 °C
Detection filters:	two Hoya U340 filters
Normalization:	none
Preheat:	220 °C (samples <5 ka) for 10 secs
Delay before measurement:	120 seconds
Equivalent dose evaluation:	single aliquot regeneration (Murray and Wintle, 2000, 2003)
Background evaluation:	black body counts <36 ct/sec, BG counts <39 ct/sec
Alpha effectiveness:	n/a
Dose-rate evaluation:	high-resolution and purity (HPGe) gamma spectrometry
Dose rate range:	4.00-4.86 Gy/ka (Grays per thousand years)
Water content:	15-20% of full saturation
Cosmic-ray contribution:	6% of total dose rate, depending on sampling site

Table 2, Appendix B. Luminescence parameters used in preparation and analyses of samples for feldspar IRSL.

Measurement parameters:	
Mineral; grain size:	polymineral: 4-11 microns
Stimulation source:	30 IR diodes, emission centered on 880 nm
Power delivered to aliquot:	17 mW/cm^2
Duration of stimulation:	100 seconds
Final signal level:	10% of initial
Photomultiplier:	Thorn-EMI 9635Q
Aliquot temperature:	30 °C IRSL
Detection filters:	390–490 (blue)
Normalization:	natural (0.5 sec)
Preheat:	124 °C for 64 hours
Delay before measurement:	24 hr or more
Equivalent dose evaluation:	additive method using integrated OSL/ satisfactory plateau
Background evaluation:	after bleaching with natural sunlight and quartz window
Alpha effectiveness:	fine grains: a = 0.07-0.09
Dose-rate evaluation:	lab and portable gamma-spectrometer
Dose rate range:	5.98-7.04 Gy/ka
Water content:	15-20% of total saturation
Cosmic-ray contribution:	6% of total dose rate, depending on sampling site

Determining the Dose Rate (D_R):

Most ionizing radiation in the sediment is from the decay of isotopes in the uranium and thorium decay chains and the radioactive potassium 40 element. The dose rate was obtained by elemental data analyses (**Table 3, A and B**). The concentrations of K, U, Th, and Rb were determined using gamma spectrometry following the procedures described in *Snyder and Duvall (2003)*. The gamma-ray spectrometer provides the isotopic discrimination of gamma rays; correspondingly, beta and alpha dose rates may be estimated. In the laboratory, the bulk samples were counted in a high-resolution and high purity gamma spectrometer fitted with a germanium detector. A table contains measured elemental concentrations, associated dose rates, and cosmic ray contributions. For each sample, estimates of cosmic-ray dose rate data are a function of depth, elevation above sea level, and geomagnetic latitude (*Prescott and Hutton, 1994*).

The bulk samples were dried, homogenized by gentle disaggregation, weighed, sealed in plastic planchets having a diameter of 15.2 cm by 3.8 cm (*some modification from Murray and others, 1987*), the samples were then immediately placed in a gamma-ray spectrometer for about 8.5 hours. Samples were then stored for a minimum of twenty-one days to allow radon to achieve radioactive equilibrium, and the measurements were repeated. We used the difference between these two spectrometer measurements to estimate the fraction of radon emanation. A sealed/unsealed ratio of <1.10 is not considered to represent significant radon escape under laboratory conditions. These count rates are accurate for calculating dose rates. We corrected alpha and beta contributions to the dose rate for grain-size attenuation (*Aitken, 1985*).

Results from luminescence dating are in **Table 4**.

Table 3, Appendix B. Elemental concentrations and dose rate calculations.

3A. Polymineral feldspars IRSL.

Sample ID	K (%)	U (ppm)	Th (ppm)	Elev. (m)	Depth (cm)	H_2O (%)	Dose Rate	D_R for K	D_R for U	D_R for Th	D_R for Rb	D_R for cosmic ray
WF-OSL-5	2.74	3.50	15.13	2650	200	20	**5.981**	2.3549	1.4821	1.8395	0.0438	0.2605
WF-OSL-4	2.42	4.14	16.64	2650	480	20	**6.078**	2.0798	1.7531	2.0230	0.0387	0.1828
WF-OSL-3	3.07	3.67	16.14	2650	140	21	**6.423**	2.6128	1.5378	1.9419	0.0486	0.2821
WF-OSL-2	2.80	3.41	16.35	2650	320	7	**7.011**	2.7593	1.6757	2.3017	0.0515	0.2230
WF-OSL-1	2.79	3.81	19.39	2650	180	15	**7.028**	2.5219	1.7039	2.4877	0.0470	0.2675

3B. Sand-grain, HF-etched, quartz for OSL.

Sample ID	K (%)	U (ppm)	Th (ppm)	Elev. (m)	Depth (cm)	H_2O (%)	Dose Rate	D_R for K	D_R for U	D_R for Th	D_R for Rb	D_R for cosmic ray
WF-OSL-5	2.74	3.50	15.13	2650	200	20	**4.114**	2.1729	0.6925	0.9443	0.0438	0.2605
WF-OSL-4	2.42	4.14	16.64	2650	480	20	**3.998**	1.9192	0.8191	1.0385	0.0387	0.1828
WF-OSL-3	3.07	3.67	16.14	2650	140	21	**4.459**	2.4109	0.7192	0.9978	0.0486	0.2821
WF-OSL-2	2.80	3.41	16.35	2650	320	7	**4.756**	2.5456	0.7717	1.1646	0.0515	0.2230
WF-OSL-1	2.79	3.81	19.39	2650	180	15	**4.704**	2.3269	0.7921	1.2707	0.0470	0.2675

Table 4, Appendix B. Feldspar IRSL and quartz OSL ages. Preferred ages in bold.

Sample unit location	Moisture (%)[a]	Feldspar Dose Rate (Gy/ka)	D_E (Gy)IRSL	Feldspar Age (ka)b	n[c]	SiO_2 Dose Rate (Gy/ka)	D_E (Gy)	Quartz Age (ka)d
WF-1 *top channel in unit 6a*	2 ± 1.5	7.04 ± 0.12	202 ± 2.10	28.7 ± 1.40	26(28)	4.86 ± 0.09	50.9 ± 0.70	**10.8 ± 0.56**
WF-2 *middle channel in unit 6a*	10 ± 1	7.03 ± 0.15	148 ± 9.92	21.3 ± 1.87	20(24)	4.70 ± 0.10	44.4 ± 0.73	**10.1 ± 0.49**
WF-3 *bottom channel in unit 6a*	8 ± 1	6.42 ± 0.12	91.2 ± 4.99 135 ± 2.55	**12.7 ± 1.46** 18.7 ± 2.96	17(20)	4.39 ± 0.08	59.6 ± 0.77	**12.0 ± 0.53**
WF-4 *Unit 1b*	8 ± 1	6.08 ± 0.11	–	–	–	4.00 ± 0.07	–	–
WF-5 *Unit 2b (top)*	14 ± 1	5.98 ± 0.08	>873 ± 166 >856 ± 214	**>147 ± 30.9** **>143 ± 37.2**	–	4.11 ± 0.06	–	–

a) Field moisture, ages based on 15-20% (sand-soil) moisture content through time as an average between field and saturation moisture values.

b) Silt fraction (4–11 micron size) for IRSL as multiple aliquot additive dose technique (MAAD). **Quoted errors are two sigma.**

c) Number of replicated equivalent dose (D_E) estimates used to calculate the mean. Figures in parentheses indicate total number of measurements, including failed runs with unusable data. Final D_E calculated from a weighted mean, which is very close to a central age model.

d) Lab used fine sand grains (250–180 micron size) for Blue-light OSL as single aliquot regeneration technique (SAR). **Quoted errors are two sigma.**

SELECTED REFERENCES, APPENDIX B

Aitken, M.J., 1985, Thermoluminescence Dating: London, Academic Press, 359 p.

Aitken, M.J., 1998, An Introduction to Optical Dating: Oxford, Oxford University Press, 267 p.

Banerjee, D., Murray, A.S., Boetter-Jensen, L., and Lang, A., 2001, Equivalent dose estimation using a single aliquot of polymineral fine grains: Radiation Measurements, v. 33, no. 1, p. 73–94.

Forman, S.L., and Pierson, J., 2002, Late Pleistocene luminescence chronology of loess deposition in the Missouri and Mississippi river valleys, United States: Palaeogeography, Palaeoclimatology, Palaeoecology, v. 186, no. 1 and 2, p. 25–46.

Galbraith, R.G., and Roberts, R.G., 2012, Statistical aspects of equivalent dose and error calculation and display in OSL dating: An overview and some recommendations: Quaternary Geochronology, v. 11, p. 1–27.

Lang, A., 1994, Infrared stimulated luminescence dating of Holocene reworked silty sediments: Quaternary Science Reviews, v. 13, no. 5-7, p. 525–528.

Mejdahl, M., 1979, Thermoluminescence Dating: Beta Dose attenuation in quartz grains: Archaeometry, v. 21, p. 61–71.

Murray, A.S., and Olley, J.M., 2002, Precision and accuracy in the optically stimulated luminescence dating of sedimentary quartz: a status review: Geochronometria, v. 21, p. 1–16.

Murray, A.S., and Wintle, A.G., 2000, Luminescence dating of quartz using an improved single-aliquot regenerative-dose protocol: Radiation Measurements, v. 32, no. 1, p. 57–73

Murray, A.S. and Wintle, A.G., 2003, The single aliquot regenerative dose protocol; potential for improvements in reliability: Radiation Measurements 37, p. 377–381.

Murray, A.S., Marten, R., Johnston, A., and Martin, P., 1987, Analysis for naturally occurring radionuclides at environmental concentrations by gamma spectrometry: Journal of Radioanalytical and Nuclear Chemistry, Article 115, p. 263–288.

Prescott, J.R. and Hutton, J.T., 1988, Cosmic ray and gamma ray dosimetry for TL and ESR: Nuclear Tracks and Radiation Measurements, v. 14, p. 223–230.

Prescott, J. R. and Hutton, J.T., 1994, Cosmic ray contributions to dose rates for luminescence and ESR dating: large depths and long-term time variations: Radiation Measurements, v. 23, p. 497–500.

Rhodes, E.J., 2011, Optically Stimulated Luminescence Dating of Sediments over the Past 200,000 Years: Annual Review of Earth and Planetary Sciences, v. 39, p. 461-488. *doi: 10.1146/annurev-earth-040610-133425.*

Richardson, C.A., McDonald, E.V. and Busacca, A.J., 1997, Luminescence dating of loess from the northwest United States: Quaternary Science Reviews, v. 16, no. 3-5, p. 403–415.

Singhvi, A.K., Sharma, Y.P. and Agrawal, D.P., 1982, Thermo-Luminescence Dating of Sand Dunes in Rajasthan, India: Nature, v. 295 (5847), p. 313–315.

Singhvi, A.K., Bluszcz, A., Bateman, M.D., and Rao, M.S., 2001, Luminescence dating of loess-palaeosol sequences and cover sands: methodological aspects and palaeoclimatic implications: Earth-Science Reviews, v. 54, no. 1-3, p. 193–211.

Snyder, S.L., and Duval, J.S., 2003, Design and construction of a gamma-ray spectrometer system for determining natural radioactive concentrations in geological samples at the U.S. Geological Survey in Reston, Virginia,: U.S. Geological Survey Open-File Report 03-29 (on-line only) *(http://pubs.usgs.gov/of/2003/of03-029)*.

Wintle, A.G., and Andrew S. Murray, 2006, A review of quartz optically stimulated luminescence characteristics and their relevance in single-aliquot regeneration dating protocols: Radiation Measurements, v. 41, p. 369–391.